Coombs, G.H., Goldberg, D.E., Klemba, M., Berry, C., Kay, J., and Mottram, J. (2001). Aspartic proteases of *Plasmodium falciparum* and other parasitic protozoa as drug targets. Trends Parasitol. *17*, 532–537.

Hamada, Y., and Kiso, Y. (2003). Protease inhibitors: design and new features. Kagaku To Seibutsu *41*, 796–803.

Kimura, T., Hidaka, K., Abdel-Rahman, H.M., Matsumoto, H., Tanaka, Y., Matsui, Y., Hayashi, Y., and Kiso, Y. (2004). Design and synthesis of dipeptide-type HIV-1 protease inhibitors with high antiviral activity. In: Peptide Science 2003, M. Ueki, ed. (Osaka, Japan: The Japanese Peptide Society), pp. 241–244.

Kiso, A., Hidaka, K., Tsuchiya, Y., Kimura, T., Hayashi, Y., Nezami, A., Liu, J., Goldberg, D.E., Freire, E., and Kiso, Y. (2004a). Dipeptide-type inhibitors targeting plasmepsins from *Plasmodium falciparum*. In: Peptide Science 2003, M. Ueki, ed. (Osaka, Japan: The Japanese Peptide Society), pp. 235–238.

Kiso, A., Hidaka, K., Kimura, T., Hayashi, Y., Nezami, A., Freire, E., and Kiso, Y. (2004b). Search for substrate-based inhibitors fitting the S2′ space of malarial aspartic protease plasmepsin II. J. Peptide Sci., in press.

Kiso, Y. (1996). Design and synthesis of substrate-based peptidomimetic human immunodeficiency virus protease inhibitors containing the hydroxymethylcarbonyl isostere. Biopolymers *40*, 235–244.

Kiso, Y., Matsumoto, H., Mizumoto, S., Kimura, T., Fujiwara, Y., and Akaji, K. (1999). Small dipeptide-based HIV protease inhibitors containing the hydroxymethylcarbonyl isostere as an ideal transition-state mimic. Biopolymers *51*, 59–68.

Macchi, B., Balestrieri, E., and Mastino, A. (2003). Effect of nucleoside-based antiretroviral chemotherapy on human T cell leukemia/lymphotropic virus type 1 (HTLV-I) infection *in vitro*. J. Antimicrob. Chemother. *51*, 1327–1330.

Maegawa, H., Kimura, T., Arii, Y., Matsui, Y., Hayashi, Y., and Kiso, Y. (2002). Identification of peptidomimetic HTLV-I protease inhibitors containing allophenylnorstatine as a transition-state isostere. In: Peptides 2002, E. Benedetti and C. Pedone, eds. (Naples, Italy: Edizioni Ziino), pp. 548–549.

Maegawa, H., Kimura, T., Arii, Y., Matsui, Y., Kasai, S., Hayashi, Y., and Kiso, Y. (2004). Identification of peptidomimetic HTLV-I protease inhibitors containing allophenylnorstatine as the transition-state mimic. Bioorg. Med. Chem. Lett., in press.

Mimoto, T., Kato, R., Takaku, H., Nojima, S., Terashima, K., Misawa, S., Kukazawa, T., Ueno, T., Sato, H., Shintani, M., Kiso, Y., and Hayashi, H. (1999). Structure-activity relationship on small-sized HIV protease inhibitors containing allophenylnorstatine. J. Med. Chem. *42*, 1789–1802.

Mimoto, T., Terashima, K., Nojima, S., Takaku, H., Nakayama, M., Shintani, M., Yamaoka, T., and Hayashi, H. (2004). Structure-activity and structure-metabolism relationships of HIV protease inhibitors containing the 3-hydroxy-2-methylbenzoyl-allophenylnorstatine structure. Bioorg. Med. Chem. *12*, 281–293.

Nezami, A., Laque, I., Kimura, T., Kiso, Y., and Freire, E. (2002). Identification and characterization of allophenylnorstatine-based inhibitors of plasmepsin II, an antimalarial target. Biochemistry *41*, 2273–2280.

Nezami, A., Kimura, T., Hidaka, K., Kiso., A., Liu, J., Kiso, Y., Goldberg, D.E., and Freire, E. (2003). High-affinity inhibition of a family of *Plasmodium falciparum* proteases by a designed adaptive inhibitor. Biochemistry *42*, 8459–8464.

Reiling, K.K., Endres, N.F., Dauber, D.S., Craik, C.S., and Stroud, R.M. (2002). Anisotropic dynamics of the JE-2147-HIV protease complex: drug resistance and thermodynamic binding mode examined in a 1.09 Å structure. Biochemistry *41*, 4582–4594.

Shuker, S.B., Mariani, V.L., Herger, B.E., and Danisson, K.J. (2003). Understanding HTLV-1 protease. Chem. Biol. *10*, 373–380.

UNAIDS and World Health Organization Report (2003). http://www.unaids.org.

Vega, S., Kang, L.-W., Velazquez-Campoy, A., Kiso, Y., Amzel, L.M., and Freire, E. (2004). A structural and thermodynamic escape mechanism from a drug resistant mutation of the HIV-1 protease. Proteins Struct. Funct. Bioinformatics *55*, 594–602.

Velazquez-Campoy, A., Kiso, Y., and Freire, E. (2001). The binding energetics of first and second-generation HIV-1 protease inhibitors: implications for drug design. Arch. Biochem. Biophys. *390*, 169–175.

Yoshimura, K., Kato, R., Yusa, K., Kavlick, M.F., Maroun, V., Nguyen, A., Mimoto, T., Ueno, T., Shintani, M., Falloon, J., et al. (1999). JE-2147: a dipeptide protease inhibitor (PI) that potently inhibits multi-PI-resistant HIV-1. Proc. Natl. Acad. Sci. USA *96*, 8675–8680.

Hamdy M. Abdel-Rahman[a],
Nawal A. El-Koussi[a],
Gamal S. Alkaramany[a],
Adel F. Youssef[a],
Yoshiaki Kiso[b]

[a] Pharmaceutical Medicinal
Chemistry Department,
Faculty of Pharmacy,
Assiut University,
Assiut 71526, Egypt
[b] Department of Medicinal
Chemistry, Kyoto
Pharmaceutical University,
Kyoto 607-8412, Japan

A Novel Dipeptide-based HIV Protease Inhibitor Containing Allophenylnorstatine

Dipeptide analogues incorporating allophenylnorstatine [Apns; (2S,3S)-3-amino-2-hydroxy-4-phenylbutyric acid] as a transition state mimic at the scissile bond were designed and synthesized in the hope of obtaining a novel KNI series of HIV protease inhibitors. The precursors, N-P_2'-3-(2S,3S)-3-(tert-butyloxy-carbonyl)amino-2-hydroxy-4-phenylbutanoyl)-5,5-dimethylthiazolidine-4-carbox-amide (N-Boc-Apns-Dmt-P_2') 4a–p were prepared by deprotection of the synthones N-P_2'-(tert-butyloxycarbonyl)-5,5-dimethylthiazolidine-4-carboxamide (Boc-Dmt-P_2') 2a–p, then coupling with (2S,3S)3-(tert-butyloxycarbonyl)amino-2-hydroxy-4-phenylbutanoic acid (N-Boc-Apns-OH) 3. The deprotected intermediates 4 were coupled with the activated carboxyl groups of the P_2 ligands to afford the target dipeptides. In this work, we fixed at the P_2 site either a 2,6-dimethylphenoxyacetyl or a 3-hydroxy-2-methylbenzoyl group. Substitutes at the P_2' site were varied to afford the members of the series 7 and 8. Improved activity of most of the members of series 8 relative to their analogues of series 7 can be partially attributed to the differences in the structures of the P_2 moieties. Positional isomerism in the P_2' moieties significantly affected the activity and polarity of the target.

Introduction

Inhibition of human immunodeficiency virus (HIV) protease is one of the most important and promising approaches for the treatment of an HIV infection.

The design and development of potent HIV protease inhibitors have generated considerable interest among the AIDS research field and HIV-positive patients. A promising class of HIV protease inhibitors containing allophenylnorstatine (Apns) as a transition state mimic yielded a series of KNI derivatives of highly potent inhibitory properties. In this work, we reported the synthesis of dipeptides with different substituents at the P_2 and P_2' positions with respect to the leads KNI-577 and KNI-901 (see Figure 1) and their protease inhibition activities.

The use of the 2,6-dimethylphenoxyacetyl moiety as P_2 ligand was already reported and provided compounds with potent HIV protease inhibitory activity

Correspondence: Nawal A. El-Koussi, Pharmaceutical Medicinal Chemistry Department, Faculty of Pharmacy, Assiut University, Assiut 71526, Egypt; Phone: +20 88 411297, Fax: +20 88 332776, e-mail: nawal-a@acc.aun.edu.eg

such as the clinically used drug ABT-378 [1, 2] (Figure 2).

On the other hand, incorporation of the 2,6-dimethylphenoxyacetyl moiety into the KNI series of inhibitors led to the development of highly potent compounds, like the dipeptide KNI-901 [3].

Further challenging of the protease inhibitory activity of the KNI series was practiced by introduction of the
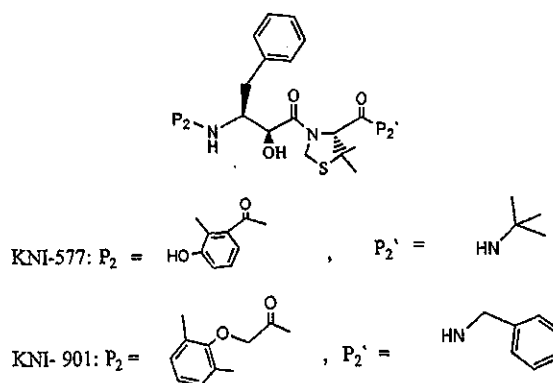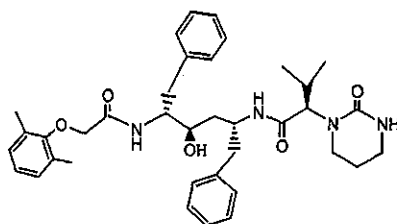

Figure 1. Lead protease inhibition of the KNI series.

588   El-Koussi et al.

Arch. Pharm. Pharm. Med. Chem. 2004, 337, 587–598

Figure 2. ABT-378 (Lopinavir).

3-hydroxy-2-methylbenzoyl moiety at P_2 sites, which simultaneously provides effective capabilities of hydrophobic and hydrogen bonding interactions with the enzyme relative sites [4].

This approach yielded the highly active KNI-577 [4–7]. The improved activity may be correlated with the combined capabilities of hydrophobic and hydrogen bonding potentialities of their intact moiety.

Guided by the leads KNI-577 and KNI-901, we prepared two series of dipeptide analogues. In one of these series, the P_2 ligand was the 2,6-dimethylphenoxyacetyl moiety as shown by compounds 7 in Table 1. Introduction of the 3-hydroxy-2-methylbenzoyl moiety at the P_2 site provided the second series of dipeptides represented by the compounds 8 in Table 2. In series 7 and 8, P_2' was changed in the hope to improve protease inhibition potential and enhance polarity. It is clear that the partition coefficient, represented by the Rt value, and solubility are closely related phenomena; therefore, the choice of moieties at P_2' with predominant polar functions was targeted in both series [8, 9].

Results and discussion

Chemistry

The target dipeptide inhibitors were prepared as illustrated in Scheme 1, starting from 5,5-dimethylthiazolidine-3-carboxylic acid (Dmt-OH), which was prepared by cyclization of L-penicillamine with formaldehyde, followed by N-protection by Boc to yield Boc-Dmt-OH 1 according to reported procedures [10]. Coupling of the amino ligands $P_2'NH_2$ with 1 in the presence of 1-hydroxybenzotriazole (HOBt) in DMF [11, 12] or diphenylphosphochloridate (DPPCl), Et_3N and AcOEt [13] afforded the intermediates 2a–p (Table 3). N-elimination of the Boc moiety and coupling with Boc-Apns-OH 3 by either 1-ethyl-3-(3'-dimethylaminopropyl) carbodiimide (EDC) or benzotriazole-1-yloxytris-(dimethylamino) phosphonium hexafluorophosphate (BOP) in the presence of HOBt in DMF [14] yielded

the synthones 4a–p (Table 4). These intermediates were used as scaffolds for the synthesis of the targets 7 and 8. 2,6-Dimethylphenoxyacetic acid 5 was activated by EDC, HOBt in DMF or THF and coupled with the deprotected 4a–n to afford the series 7a–n (Table 1). In series 8, 3-acetyl-2-methylbenzoic acid 6 was activated by DPPCl in AcOEt and then coupled with the deprotected synthones 4a–h, o and p. Hydrolytic cleavage of the 3-acetyl group by LiOH yielded 8a–h, o and p dipeptides in Table 2. The final compounds obtained after crystallization were checked by analytical HPLC; from the resulting data, preparative HPLC was established and carried out. The purity was checked again by analytical HPLC. The fractions were mixed and lyophilized to afford the analytically pure final compounds; yields of the products were determined by reversed-phase HPLC (RP-HPLC). Within each series, the parallelism between Rt of the compounds and the polarity of the P_2' moieties could be easily observed. The effect of the location of the polar groups in the P_2' moieties on the Rt values of the positional isomers 7g, h, i, k, l, m, n and in 8g, h, o, p was perceptible. Homogenity of targets 7 and 8 was checked by TLC using two systems of different polarities: chloroform/methanol (10:1) and chloroform/methanol/water (8:3:1).

### Structure activity relationship against HIV-1 protease

The effect of variation of the P_2' moieties on HIV-1 protease inhibition of the potent leads KNI-901 and KNI-577 was regarded as the main objective of the present study. The benzylamino group at the P_2' site in KNI-901 was the target modified to afford the dipeptides 7, whereas the t-butyl group at the P_2' site in KNI-577 was replaced by the same modified benzylamino derivatives to afford almost all members of series 8.

Three approaches were considered for modification of the benzylamine moiety. First, the assumption that the phenyl ring must be distanced by one atom from the amidic NH represents an essential requisite. Groups of different bulkiness and polarity, with one atom bridging the phenyl ring and the amidic NH, were inserted to replace the α-methylene group in benzylamine. This approach was challenged by the compounds 7a, b, e and 8a, b, e. As shown in Table 5, compounds 7b and 8b with inserted α-N (CH_3) were the least active ones. On the other hand, the 2-isopropylene bridge significantly improved the activity of 7a and 8a, which are still less active than the corresponding leads. Compound 8e revealed 91.2% inhibition potential, which is higher than the potential of the lead KNI-577. Matching the activities of 7a, e with their analogues 8a, e dem-

Arch. Pharm. Pharm. Med. Chem. 2004, 337, 587–598

A Novel Dipeptide-based HIV Protease Inhibitor 589

onstrated a boosting effect of the P_2 moiety in series 8. Secondly, introduction of a polar substitute at the *o-*, *m-*, o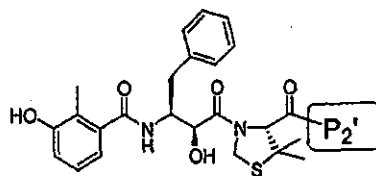r *p*-position on the benzene ring was tried by preparing **7c, d, f, k–n** and **8c, d, f** dipeptides. All *these isomers* were less active than the leads; however, the derivatives of the **8** series still revealed a

Table 1. Physical data of dipeptide-based HIV protease inhibitors **7**.
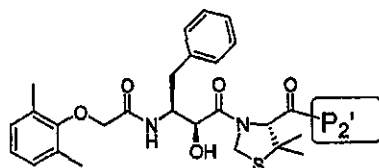
No.	P_2'	mp (°C)	Yield (%)	HPLC[§] Rt (min)	TLC Rf_1[†]	Rf_2[¥]
7a		89–90	85	27.44	0.98	0.96
7b		115–117	54.5	24.81	0.81	0.90
7c		89–91	65	26.37	0.68	0.89
7d		85–88	71	27.12	0.72	0.90
7e[#]		103–105	61	27.28	0.90	0.96
7f		110–113	78	25.08	0.90	0.93
7g		107–108	71	16.92	0.80	0.86
7h		141–143	70	17.34	0.62	0.77
7i		98–100	73	18.10	0.68	0.84
7j		149–151	55	21.10	0.62	0.77
7k		124–126	79	20.38	0.54	0.83
7l		98–100	53	24.70	0.84	0.91
7m		140–142	57	19.81	0.52	0.90
7n		99–100	63	24.38	0.89	0.94

[#] Mixture of diastereomers; [§] 20–80% CH_3CN in 0.1% aqueous TFA over 30 min; [†] $CHCl_3/CH_3OH$ (10:1); [¥] $CHCl_3/CH_3OH/H_2O$ (8:3:1).

590   El-Koussi et al.

Arch. Pharm. Pharm. Med. Chem. 2004, 337, 587–598

Table 2. Physical data of dipeptide-based HIV protease inhibitors **8**.

No.	$P_2{'}$	mp (°C)	Yield (%)	HPLC[§] Rt (min)	TLC	
					Rf_1[†]	Rf_2[*]
8a		128–130	65.5	20.86	0.69	0.88
8b		150–152	78	18.08	0.37	0.76
8c		127–129	68	19.45	0.57	0.83
8d		121–123	72	21.10	0.67	0.86
8e[#]		139–141	58	20.42 20.52	0.56	0.76
8f		139–140	71	20.24	0.59	0.67
8g		141–143	35.5	11.47	0.58	0.80
8h		154–156	24	9.94	0.35	0.65
8o		153–155	76	27.15	0.56	0.66
8p		159–161	66	26.64	0.54	0.70

[#], [§], [†] and [*] as in Table 1.

higher pattern of activity that can only be attributed to the different P_2 moieties. Finally, the benzyl moiety was replaced by the bioisosteric α-, β-, and γ-picolines. This approach yielded the most active derivative **7g**, which is equally active as the lead KNI-901, with an apparently enhanced polarity. Improvement of polarity presumably may advantageously affect its absorption and distribution properties. Furthermore, the presence of a basic pyridine center allows for formation of salts.

The significantly reduced activity of the α-picolinyl derivative **7l** may be attributed to the possible competition for intramolecular hydrogen bond formation between the pyridine N and the amidic NH, which participates in a crucial hydrogen bonding with the water molecule bridging Ala28 and Asp29 in the $S_2{'}$ site of the enzyme [15]. In the absence of such interaction, higher activity of the β- and γ-picoline **7g** and **7h** was observed. On the other hand, the lowered activity of the alkoxy **7c**, **d**, **8c**, **d** and 4,6-dimethyl-1,2-dihydro-3-
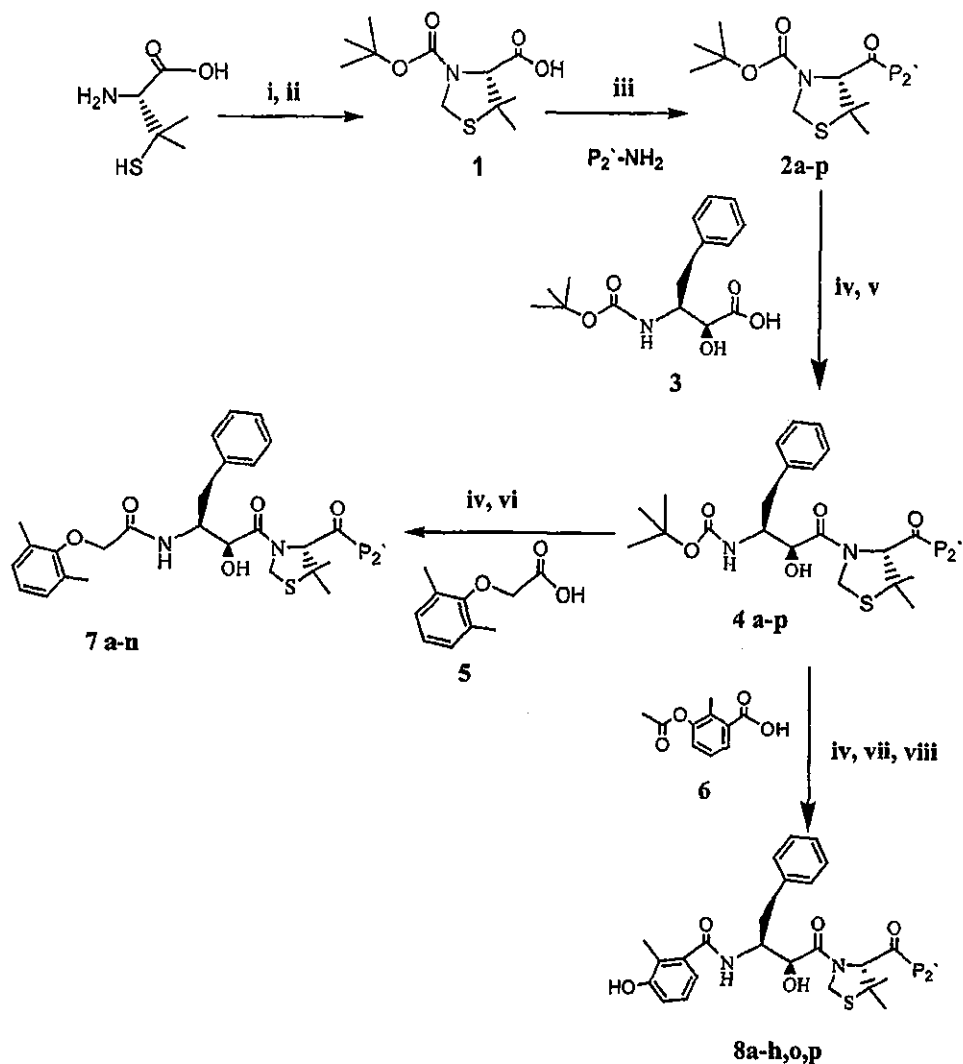
(i) aq 37% HCHO (ii) (Boc)₂O   (iii) HOBt in DMF or DPPCl, Et₃N, AcOEt (iv) N HCl/dioxane

(v) EDC, HOBt in DMFor BOP, HOBt in DMF (vi) EDC, HOBt in DMFor THF

(vii) DPPCl in AcOEt, (viii) LiOH

Scheme 1. Synthesis of dipeptides **7** and **8**.

picolinyl-2- one **7j** can be equally attributed to possible intramolecular hydrogen bonding between the unshared pair of electrons on the o-oxygen and the amidic NH.

Positional isomers of the substituted benzyl amines and of the picolines revealed a significant impact on activity. The β-picolinyl **7g**, and **8g** and the m-substituted benzyl derivatives **7k, l** on the one hand exerted

592 El-Koussi et al.

Arch. Pharm. Pharm. Med. Chem. 2004, 337, 587–598

Table 3. Physical data of intermediate compounds N-Boc-Dmt-P$_2'$ **2**.

No.	P$_2'$	mp (°C)	HPLC[§] Rt (min)	No.	P$_2'$	mp (°C)	HPLC[§] Rt (min)
2a		102–104	23.24	2i		116–119	10.29
2b		185–188	19.71	2j		128–130	13.30
2c		112–113	23.34	2k		88–89	13.48
2d		113–114	22.92	2l	‡		20.14
2e[#]		60–62	23.92 24.16	2m		107–109	13.92
2f		124–126	21.68	2n		115–116	20.96
2g		‡	7.68	2o		155–156	30.56
2h		162–164	9.86	2p		178–179	30.10

[#] Mixture of diastereomers; [§] 20–80% CH_3CN in 0.1% aqueous TFA over 30 min; ‡ not determined, sticky semisolid material.

a relatively higher activity when matched with the γ-picolines **7h**, and **8h** and the *p*-substituted benzyls **7m, n** on the other hand. A common feature of these isomers is the availability of an atom or group on the aromatic ring that carries an unshared pair of electrons. It seems feasible to correlate the observed differences in activity with the unshared pair of electrons that should be suitably oriented at a critical distance from the amidic NH. Deviation from this critical distance might lead to decreased activity. Thus, a location of the unshared pair of electrons separated by three carbons from the amidic NH seems to give the optimum activity, as in **7g**. Shifting of the unshared pair of electrons on N towards α- or γ-positions either gets it involved in intramolecular hydrogen bonding, as in **7l**, or diminishes its supporting role of interaction with the enzyme, as in **7h**. By analogy, the differences in activities of the *m*- and *p*-isomers of benzylcarboxamides **7k** and **7m** and the methyl benzylcarboxylates **7l** and **7n** were found to parallel the distance separating the carbonyl oxygen from the amidic NH.

The tolerance of the S$_2'$ site to accommodate a bulky substituent was challenged by the attachment of 1- or 2- adamantyl groups, which can be regarded as the constrained analogues of the tert-butyl moiety at the P$_2'$ position in the lead KNI-577. The yielded dipeptides **8o** and **8p** were found to be the least active derivatives.

Conclusions

KNI-577 and KNI-901 leads are substrate-based HIV protease inhibitors. The two leads are members of the KNI series containing allophenylnorstatine (Apns) with hydroxymethylcarbonyl isostere as a transition state mimic at the scissile peptide bond.

The activity of the prepared series of P$_2$-Apns-Dmt-P$_2'$ strongly depends on the simultaneous balance between electronic and steric properties of both the P$_2$ and P$_2'$ moieties. As shown from Table 5, the ability of interaction of P$_2$ and P$_2'$ with the relevant enzyme

Arch. Pharm. Pharm. Med. Chem. 2004, 337, 587–598

A Novel Dipeptide-based HIV Protease Inhibitor   593

Table 4. Physical data of intermediate compounds N-Boc-Dmt-P$_2$' **4.**

No.	P$_2$'	mp (°C)	HPLC[§] Rt (min)	No.	P$_2$'	mp (°C)	HPLC[§] Rt (min)
4a	(structure)	102–106	25.56	**4i**	(structure, pyridyl)	94–98	15.52
4b	(structure, N-CH$_3$)	106–109	22.72	**4j**	(structure, OH, pyridine)	147–150	18.87
4c	(structure, O–)	99–102	23.70	**4k**	(structure, CONH$_2$)	132–135	18.80
4d	(structure, O-ethyl)	100–103	25.57	**4l**	(structure, COOCH$_3$)	117–120	25.44
4e[#]	(indane structure)	95–98	25.06 25.23	**4m**	(structure, CONH$_2$)	96–99	17.78
4f	(benzodioxole structure)	75–78	25.66	**4n**	(structure, COOCH$_3$)	110–112	22.66
4g	(pyridyl structure)	96–100	16.19	**4o**	(adamantyl structure)	103–106	32.75
4h	(pyridyl structure)	105–109	14.92	**4p**	(adamantyl structure)	107–109	31.94

[#] and [§] as in Table 3.

sites S$_2$ and S$_2$' would significantly affect the fitting of Apns to the enzyme catalytic site, which reflects the HIV protease inhibitory activity.

Two derivatives were found to be equally or more active than the leads KNI-577 and KNI-901 and present promising candidates for further investigations.

Experimental

Melting points were determined on a micro hot plate of a Yanaco micro melting point apparatus and were uncorrected. The optical rotations were measured on a Horiba model SEPA-300 digital polarimeter. TLC was performed on precoated Merck silica gel 60 F$_{254}$ sheets. Column chromatography was carried out on Merck silica gel 60 (particle size 0.063–0.200 mm).

Analytical RP-HPLC was performed with a Hitachi L-7100 pump and an L-7400 UV detector utilizing YMC Pack ODS-AM AM 302.

Preparative RP-HPLC was performed with a Shimadzu LC-4A liquid chromatograph utilizing a YMC Pack ODS-AM type SH-343-5AM column (250 × 20 mm i.d., S-5 μm, 120 A).
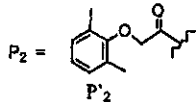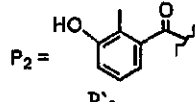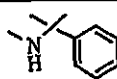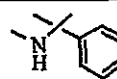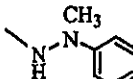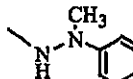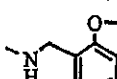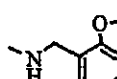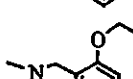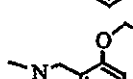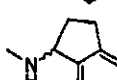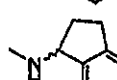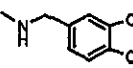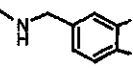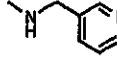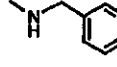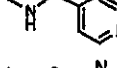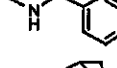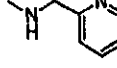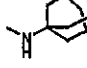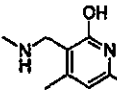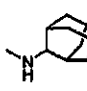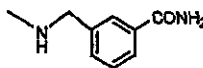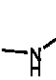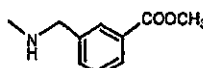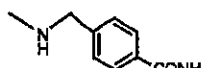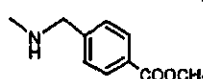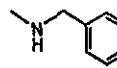
^{1}H NMR spectra were recorded on a JEOL JNM-EX 270 (270 MHz) spectrometer. Chemical shifts are given in (δ ppm) relative to tetramethylsilane (TMS) as an internal standard. 13C NMR spectra were recorded on a JEOL JNM-EX 270 (67.5 MHz) using solvents as internal standard. FAB mass spectra (FAB-MS) and high-resolution FAB-MS (HRFAB-MS) were recorded on a JEOL JMS-SX102 AQQ/MS-HYB10 mass spectrometer using glycerol, thioglycerol or Magic Bullet as internal references. MALDI TOF mass spectra were measured at Voyager-DE^{TM}RP Biospectrometry^{TM} Workstation (Per-Septive Biosystems). Commercially available chemicals were purchased from Nacalai tesque, Waku Chemicals or Tokyo Chemical industries, Japan, and were used without further purification. Commercially non-available chemicals were prepared according to standard methods described in [16] and showed 1H NMR and 13C NMR spectra in accordance with the assigned structures.

(tert-Butyloxycarbonyl)-5,5-dimethylthiazolidine-4-carboxylic acid Boc-Dmt-OH (1) [10]

Yield 81%, mp 124–127°C.

N-P$_2$'-(tert-Butyloxycarbonyl)-5,5-dimethylthiazolidine-4-carboxamide Boc-Dmt-P$_2$' (2a–p)

Table 5. HIV protease inhibitory activity of targeted dipeptides P$_2$-Apns-Dmt-P$_2'$ **7** and **8**.

No.	P$_2$ = (structure) P'$_2$	% HIV protease inhibition (50 nM)	No.	P$_2$ = (structure) P'$_2$	% HIV protease inhibition (50 nM)
7a		72.5	8a		82.2
7b		15.3	8b		12.9
7c		24.0	8c		65.8
7d		41.7	8d		49.7
7e[#]		64.5	8e[#]		91.2
7f		27.6	8f		67.6
7g		86.8	8g		62.6
7h		70.7	8h		34.5
7i		57.8	8o		7.1
7j		20.9	8p		5.5
7k		67.7	KNI-577		87.6
7l		45.0			
7m		3.3			
7n		28.6			
KNI-901		86			

mixture of diasteromers.

Arch. Pharm. Pharm. Med. Chem. 2004, 337, 587–598

A Novel Dipeptide-based HIV Protease Inhibitor   595

Boc-Dmt-OH (1.5 g, 5.74 mmol) was dissolved and stirred in AcOEt (20 mL); Et₃N (0.88 mL, 6.33 mmol) and DPPCl (1.31 mL, 6.33 mmol) were added at 0 °C. The mixture was stirred at room temperature for 1 h, then appropriate amine (6.33 mmol) and Et₃N (0.88 mL, 6.33 mmol) were added. Stirring was continued at room temperature for 6 h. The mixture was washed twice with 10 % citric acid, 5 % NaHCO₃ and brine, dried over anhydrous Na₂SO₄ and filtered. The filtrate was evaporated under reduced pressure, crystallized from n-hexane and dried in a dessicator [16, 17].

(2S,3S)3-(tert-Butyloxycarbonyl)amino-2-hydroxy-4-phenyl-butanoic acid N-Boc-Apns-OH (3) [18]

Yield 8 %, mp147–148 °C.

N-P₂'-3-(2S,3S)-3-(tert-butyloxycarbonyl)amino-2-hydroxy-4-phenylbutanoyl)-5,5-dimethylthiazolidine-4-carboxamide Boc-Apns-Dmt-P₂' (4a–p)

To the appropriate Boc-Dmt-P₂' 2a–p (0.5 mmol) in 4 N HCl/dioxane solution (2 mL), anisol (108 µL, 1 mmol) was added at 0 °C. This solution was stirred for 2 h at room temperature. The solvent was evaporated in vacuo, ether was added, the mixture was centrifuged, and the residue was dissolved in DMF (5 mL). Boc-Apns-OH 3 (134 mg, 0.45 mmol), HOBt. H₂O (76.6 mg, 0.5 mmol), BOP (211 mg, 0.5 mmol) and Et₃N (139 mL, 1 mmol) were added at 0 °C. The mixture was stirred overnight at room temperature. The solvent was then removed under vacuum and the residue was extracted with AcOEt. The organic layer was washed with 10 % citric acid, 5 % NaHCO₃ and brine, dried over anhydrous Na₂SO₄ and filtered. The filtrate was evaporated under reduced pressure. The residue was purified by column chromatography, and the appropriate fractions were pooled and evaporated to yield the coupled peptide (Boc-Apns-Dmt-P₂'), which was dried in a desiccator [16, 17].

2,6-Dimethylphenoxyacetic acid (5)

Compound 5 was synthesized starting from 2,6-dimethyl phenol by alkylation with ethyl-2-bromoacetate, then hydrolysis. Yield 37 %, mp138–139 °C.

3-Hydroxy-2-methylbenzoic acid [16]

Yield 86.5 %, mp142–144 °C.

3-Acetyloxy-2-methylbenzoic acid (6)

Acetylation of 3-hydroxy-2-methylbenzoic acid yielded 3-acetyloxy-2-methylbenzoic acid 6 (quantitative, mp 147–148 °C).

Synthesis of dipeptides containing 2,6-dimethyl phenoxyacetic acid as P₂ ligand (2,6-dimethylphenoxyacetyl-Apns-Dmt-P₂') (7a–n)

The titled compounds were prepared, starting from N-Boc-Apns-Dmt-P₂' 4a–n (20.8 mmol) in 4 N HCl/dioxane (40 mL); anisole (4.5 mL, 41.67 mmol) was added at 0 °C. The reaction mixture was stirred for 1 h at room temperature, and the solvent was then removed in vacuo at room temperature; ether was added, and the mixture was centrifuged. The formed precipitate was dissolved in DMF (40 mL), and then 2,6-dimethylphenoxyacetic acid 5 (22.85 mmol), HOBt.H₂O (3.5 g, 22.85 mmol), EDC.HCl (4.3 g, 22.43 mmol) and Et₃N (5.78 mL, 41.6 mmol) were added at 0 °C. The reaction mixture was stirred

overnight at room temperature, and the solvent was removed under reduced pressure. The residue was extracted with Ac-OEt. The organic layer was washed with 10 % citric acid, 5 % NaHCO₃ and brine, dried over anhydrous Na₂SO₄, filtered and evaporated. The residue was crystallized from n-hexane. Physical data are listed in Table 1.

2,6-Dimethylphenoxyacetyl-Apns-Dmt-NH-cumyl (7a)

[a]ᴰ⁸ −1.60 (c = 0.218, CH₃OH), ¹H NMR (DMSO-d₆) δ: 1.43 (s, 3H), 1.49 (s, 1H), 1.54 (s, 3H), 1.65 (s, 3H), 2.16 (s, 6H), 2.70–2.73 (m, 2H), 3.99–4.05 (d, J = 14.51 Hz, 1H), 4.14–4.20 (d, J = 13.85 Hz, 1H), 4.28 (bs, 1H), 4.42 (s, 1H), 4.66 (s, 1H), 4.84–4.93 (m, 2H), 6.92–7.02 (m, 3H), 7.15–7.24 (m, 10H), 7.41–7.44 (d, J = 7.69 Hz, 1H), 8.24–8.27 (d, J = 8.58 Hz, 1H), HRFAB-MS: m/z 618.3004 for [M+H]⁺ (calcd. 618.3002 for C₃₅H₄₄N₃O₅S).

2,6-Dimethylphenoxyacetyl-Apns-Dmt-NH-MPH (7b)

[a]ᴰ⁴·⁹ −11.42 (c = 0.07, CH₃OH), ¹H NMR (DMSO-d₆) δ: 1.49 (s, 3H), 1.58 (s, 3H), 2.16 (s, 6H), 2.76–2.82 (m, 2H), 3.97–4.02 (d, J = 13.53 Hz, 1H), 4.15–4.20 (d, J = 13.52 Hz, 1H), 4.26–4.48 (m, 3H), 4.97–5.00 (m, 2H), 6.68–6.71 (t, J = 7.26 Hz, 1H), 6.81–7.03 (m, 4H), 7.12–7.25 (m, 8H), 8.17–8.20 (d, J = 8.91 Hz, 1H), 10.17 (s, 1H), HRFAB-MS: m/z 605.2804 for [M+H]⁺ (calcd. 605.2798 for C₃₃H₄₁N₄O₅S).

2,6-Dimethylphenoxyacetyl-Apns-Dmt-NH-(2-OCH₃)Bz (7c)

[a]ᴰ⁴ −14.85 (c = 0.202, CH₃OH), ¹H NMR (DMSO-d₆) δ: 1.34 (s, 3H), 1.50 (s, 3H), 2.14 (s, 6H), 2.77–2.80 (m, 2H), 3.77 (s, 3H), 3.97–4.02 (d, J = 14.19 Hz, 1H), 4.13–4.18 (d, J = 14.18 Hz, 1H), 4.25–4.27 (d, J = 5.28 Hz, 2H), 4.37–4.40 (m, 1H), 4.46–4.49 (m, 2H), 4.91–5.00 (m, 2H), 6.79–6.85 (t, J = 7.59 Hz, 1H), 6.89–7.01 (m, 2H), 7.15–7.30 (m, 9H), 8.12–8.15 (d, J = 8.57 Hz, 1H), 8.27–8.35 (t, J = 5.6 Hz, 1H), HRFAB-MS: m/z 620.2854 for [M+H]⁺ (calcd. 620.2794 for C₃₄H₄₂N₃O₆S).

2,6-Dimethylphenoxyacetyl-Apns-Dmt-NH-(2-OC₂H₅)Bz (7d)

[a]ᴰ⁷·³ −9.96 (c = 0.158, CH₃OH), ¹H NMR (DMSO-d₆) δ: 1.31–1.35 (m, 6H), 1.51 (s, 3H), 2.14 (s, 6H), 2.77–2.80 (m, 2H), 3.93–4.05 (m, 3H), 4.12–4.18 (m, 1H), 4.26–4.28 (d, J = 4.29 Hz, 2H), 4.39 (s, 1H), 4.47–4.50 (m, 2H), 4.92–5.00 (m, 2H), 6.78–6.83 (t, J = 6.27 Hz, 1H), 6.90–7.01 (m, 3H), 7.12–7.30 (m, 7H), 8.13–8.15 (d, J = 7.91 Hz, 1H), 8.30 (t, J = 5.6 Hz, 1H), HRFAB-MS: m/z 634.2969 for [M+H]⁺ (calcd. 634.2951 for C₃₅H₄₄N₃O₆S).

2,6-Dimethylphenoxyacetyl-Apns-Dmt-NH-Ind (7e)

[a]ᴰ⁵ +19.86 (c = 0.448, CH₃OH), ¹H NMR (DMSO-d₆) δ: 1.44 (s, 3H), 1.51 (s, 3H), 1.79–1.84 (m, 1H), 2.15 (s, 6H), 2.34–2.40 (m, 1H), 2.81–2.91 (m, 4H), 3.95–4.02 (m, 1H), 4.16–4.22 (m, 1H), 4.39–4.50 (m, 3H), 4.98–4.99 (m, 2H), 5.32–5.35 (m, 1H), 6.90–7.08 (m, 4H), 7.17–7.38 (m, 8H), 8.14–8.17 (d, J = 8.24 Hz, 1H), 8.35–8.45 (dd, J = 8.24 Hz, 1H), HRFAB-MS: m/z 616.2878 for [M+H]⁺ (calcd. 616.2845 for C₃₅H₄₂N₃O₅S), TOF-MS 616.727 for [M+H]⁺.

2,6-Dimethylphenoxyacetyl-Apns-Dmt-NH-Pip (7f)

[a]ᴰ⁷ −2.00 (c = 0.15, CH₃OH), ¹H NMR (DMSO-d₆) δ: 1.34 (s, 3H), 1.51 (s, 3H), 2.15 (s, 6H), 2.76–2.80 (m, 2H), 3.99–4.02 (m, 1H), 4.14–4.29 (m, 3H), 4.34–4.48 (m, 3H),

596   El-Koussi et al.

Arch. Pharm. Pharm. Med. Chem. 2004, 337, 587–598

4.97 (s, 2H), 5.88–5.92 (m, 2H), 6.77 (s, 2H), 6.85 (s, 1H), 6.95–7.02 (m, 3H), 7.19–7.30 (m, 4H), 8.09–8.13 (d, J = 9.17 Hz, 1H), 8.43–8.48 (t, J = 6.11 Hz, 1H), HRFAB-MS: m/z 634.2583 for [M+H]+ (calcd. 634.2587 for $C_{34}H_{40}N_3O_7S$).

2,6-Dimethylphenoxyacetyl-Apns-Dmt-NH-3-picolyl (7g)

$[\alpha]_D^{23.8}$ +47.14 (c = 0.28, CH$_3$OH), ^{1}H NMR (DMSO-d$_6$) δ: 1.34 (s, 3H), 1.53 (s, 3H), 2.12 (s, 6H), 2.76–2.84 (m, 2H), 3.93–3.98 (d, J = 14.19 Hz, 1H), 4.11–4.17 (d, J = 14.19 Hz, 1H), 4.19–4.72 (m, 5H), 5.00 (m, 2H), 6.89–7.01 (m, 3H), 7.16–7.24 (m, 5H), 7.63–7.68 (m, 1H), 8.07–8.11 (d, J = 8.91 Hz, 1H), 8.14–8.17 (d, J = 7.59 Hz, 1H), 8.57–8.58 (d, J = 3.96 Hz, 1H), 8.67 (s, 1H), 8.72–8.80 (t, J = 5.6 Hz, 1H), HRFAB-MS: m/z 591.2639 for [M+H]+ (calcd. 591.2641 for $C_{32}H_{39}N_4O_5S$). TOF-MS 591.543 for [M+H]+.

2,6-Dimethylphenoxyacetyl-Apns-Dmt-NH-4-picolyl (7h)

$[\alpha]_D^6$ +36.36 (c = 0.55, CH$_3$OH), ^{1}H NMR (DMSO-d$_6$) δ: 1.37 (s, 3H), 1.55 (s, 3H), 2.12 (s, 6H), 2.71–2.89 (m, 2H), 3.93–3.98 (d, J = 14.19 Hz, 1H), 4.09–4.15 (d, J = 14.19, 1H), 4.32–4.61 (m, 5H), 5.00 (s, 2H), 6.89–7.01 (m, 3H), 7.12–7.26 (m, 5H), 7.63–7.66 (d, J = 5.74 Hz, 2H), 8.09–8.13 (d, J = 9.24 Hz, 1H), 8.58–8.61 (d, J = 6.26 Hz, 2H), 8.77–8.81 (t, J = 5.94 Hz, 1H), HRFAB-MS: m/z 591.2628 for [M+H]+ (calcd. 591.2641 for $C_{32}H_{39}N_4O_5S$).

2,6-Dimethylphenoxyacetyl-Apns-Dmt-NH-2-picolyl (7i)

$[\alpha]_D^5$ +21.80 (c = 0.61, CH$_3$OH), ^{1}H NMR (DMSO-d$_6$) δ: 1.37 (s, 3H), 1.54 (s, 3H), 2.13 (s, 6H), 2.76–2.85 (m, 2H), 3.95–4.00 (d, J = 14.19 Hz, 1H), 4.12–4.17 (d, J = 14.19 Hz, 1H), 4.26–4.56 (m, 5H), 4.94–5.02 (q, J = 9.24 Hz, 2H), 6.89–7.01 (m, 3H), 7.12–7.26 (m, 5H), 7.32–7.37 (t, J = 6.6 Hz, 1H), 7.53–7.56 (d, J = 7.59 Hz, 1H), 7.81–7.87 (t, J = 7.58 Hz, 1H), 8.11–8.14 (d, J = 8.57 Hz, 1H), 8.53–8.54 (d, J = 4.62 Hz, 1H), 8.71–8.75 (t, J = 5.94 Hz, 1H), HRFAB-MS: m/z 591.2631 for [M+H]+ (calcd. 591.2641 for $C_{32}H_{39}N_4O_5S$).

2,6-Dimethylphenoxyacetyl-Apns-Dmt-NH-(2-hydroxy-4,6-dimethyl)-3-picolyl (7j)

$[\alpha]_D^{6.3}$ –4.28 (c = 0.07, CH$_3$OH), ^{1}H NMR (DMSO-d$_6$) δ: 1.31 (s, 3H), 1.45 (s, 3H), 2.05–2.24 (m, 12H), 2.73–2.80 (m, 2H), 3.98–4.20 (m, 4H), 4.29–4.40 (bs, 1H), 4.44–4.50 (m, 2H), 4.93 (m, 2H), 5.74 (s, 1H), 6.91–7.06 (m, 3H), 7.13–7.37 (m, 5H), 7.98–8.02 (t, J = 5.6 Hz, 1H), 8.13–8.16 (d, J = 7.71 Hz, 1H), HRFAB-MS: m/z 635.2897 for [M+H]+ (calcd. 635.2903 for $C_{34}H_{43}N_4O_6S$).

2,6-Dimethylphenoxyacetyl-Apns-Dmt-NH-Bz(3-CONH₂) (7k)

$[\alpha]_D^6$ +42.66 (c = 0.075, CH$_3$OH), ^{1}H NMR (DMSO-d$_6$) δ: 1.34 (s, 3H), 1.51 (s, 3H), 2.14 (s, 6H), 2.71–2.80 (m, 2H), 3.96–4.02 (d, J = 14.19 Hz, 1H), 4.14–4.18 (d, J = 14.19 Hz, 1H), 4.24–4.49 (m, 5H), 4.94–5.03 (m, 2H), 6.90–7.05 (m, 3H), 7.15–7.34 (m, 6H), 7.44–7.48 (d, J = 6.6 Hz, 1H), 7.68–7.70 (d, J = 7.58 Hz, 1H), 7.81 (s, 1H), 7.93 (s, 2H), 8.09–8.13 (d, J = 9.24 Hz, 1H), 8.55–8.62 (t, J = 5.8 Hz, 1H), HRFAB-MS: m/z 633.2756 for [M+H]+ (calcd. 633.2747 for $C_{34}H_{41}N_4O_6S$).

2,6-Dimethylphenoxyacetyl-Apns-Dmt-NH-Bz(3-COOCH₃) (7l)

$[\alpha]_D^4$ –13.33 (c = 0.03, CH$_3$OH), ^{1}H NMR (DMSO-d$_6$) δ: 1.33 (s, 3H), 1.51 (s, 3H), 2.13 (s, 6H), 2.75–2.79 (m, 2H), 3.81 (s, 3H), 3.96–4.02 (d, J = 14.19 Hz, 1H), 4.13–4.17 (d, J = 14.19 Hz, 1H), 4.30–4.52 (m, 5H), 4.96–4.98 (m, 2H), 5.50–5.53 (d, J = 8.7 Hz, 1H), 6.92–7.01 (m, 3H), 7.19–7.26 (m, 5H), 7.36–7.42 (t, J = 7.2 Hz, 1H), 7.57–7.61 (d, J = 6.6 Hz, 1H), 7.75–7.78 (d, J = 7.58 Hz, 1H), 7.91 (s, 1H), 8.09–8.12 (d, J = 8.25 Hz, 1H), 8.58–8.62 (t, J = 5.8 Hz, 1H), HRFAB-MS: m/z 648.2753 for [M+H]+ (calcd. 648.2743 for $C_{35}H_{42}N_3O_7S$).

2,6-Dimethylphenoxyacetyl-Apns-Dmt-NH-Bz(4-CONH₂) (7m)

$[\alpha]_D^5$ +22.00 (c = 0.05, CH$_3$OH), ^{1}H NMR (DMSO-d$_6$) δ: 1.35 (s, 3H), 1.52 (s, 3H), 2.14 (s, 6H), 2.77–2.89 (m, 2H), 3.96–4.03 (m, 1H), 4.15–4.20 (m, 1H), 4.26–4.52 (m, 5H), 5.00 (s, 2H), 6.90–7.03 (m, 3H), 7.15–7.33 (m, 5H), 7.35–7.40 (d, J = 7.2 Hz, 2H), 7.76–7.81 (d, J = 7.2 Hz, 2H), 7.89 (s, 2H), 8.10–8.15 (d, J = 8.1 Hz, 1H), 8.55–8.60 (t, J = 5.4 Hz, 1H), HRFAB-MS: m/z 633.2763 for [M+H]+ (calcd. 633.2747 for $C_{34}H_{41}N_4O_6S$).

2,6-Dimethylphenoxyacetyl-Apns-Dmt-NH-Bz(4-COOCH₃) (7n)

$[\alpha]_D^6$ +16.66 (c = 0.202, CH$_3$OH), ^{1}H NMR (DMSO-d$_6$) δ: 1.35 (s, 3H), 1.52 (s, 3H), 2.14 (s, 6H), 2.76–2.79 (m, 2H), 3.81 (s, 3H), 3.96–4.01 (d, J = 14.19 Hz, 1H), 4.13–4.19 (d, J = 14.51 Hz, 1H), 4.29–4.48 (m, 5H), 4.98 (s, 2H), 6.90–7.01 (m, 3H), 7.18–7.24 (m, 5H), 7.43–7.46 (d, J = 7.26 Hz, 2H), 7.82–7.85 (d, J = 8.24 Hz, 2H), 8.11–8.15 (d, J = 8.75 Hz, 1H), 8.63 (t, J = 5.4 Hz, 1H), HRFAB-MS: m/z 648.2753 for [M+H]+ (calcd. 648.2743 for $C_{35}H_{42}N_3O_7S$).

Dipeptides containing the 3-hydroxy-2-methylbenzoyl moiety (3-hydroxy-2-methyl benzoyl-Apns-Dmt-P₂′) (8a–h, o, p)

To a solution of the appropriate Boc-Apns-Dmt-P₂′ **4a–h, o, p** (0.1 mmol) in 4 N HCl/dioxane solution (1 mL), anisole (22 μL, 0.2 mmol) was added at 0 °C. The reaction mixture was stirred for 1 h at room temperature. The solvent was removed in vacuum at room temperature; ether was added. After centrifugation, the residue was suspended in AcOEt (5 mL), then Et₃N (17 μL, 0.12 mmol) was added (solution A). 3-Acetyloxy-2-methylbenzoic acid **6** (21.3 mg, 0.11 mmol) was dissolved in AcOEt (5 mL), then Et₃N (17 μL, 0.12 mmol) and DPPCl (25 μL, 0.12 mmol) were added at 0 °C. The mixture was stirred at room temperature for 1 h, then mixed with solution A. The mixture was further stirred at room temperature for 6 h, then washed with 10 % citric acid, 5 % NaHCO₃ and brine. The organic layer was dried and evaporated under reduced pressure. The residue was dissolved in methanol (2 mL), then 1 M LiOH (3 mL) was added. Stirring was continued at room temperature for 5 h, followed by addition of 10 % citric acid till pH 3. The mixture was extracted with AcOEt and washed with 10 % citric acid and brine. The organic extract was dried, evaporated and crystallized from n-hexane. The crude product was purified using analytical, preparative and analytical HPLC. The pure product was lyophilized. Physical data are listed in Table 2.

3-Hydroxy-2-methylbenzoyl-Apns-Dmt-NH-cumyl (8a)

$[\alpha]_D^{3.5}$ +18.69 (c = 0.23, CH$_3$OH), ^{1}H NMR (DMSO-d$_6$) δ: 1.43 (s, 3H), 1.50 (s, 3H), 1.53 (s, 3H), 1.65 (s, 3H), 1.82 (s, 3H), 2.71 (m, 2H), 4.20–4.38 (m, 2H), 4.50–5.51 (d, J = 2.97 Hz,

1H), 4.65 (s,1H), 4.93–4.97 (d, J = 8.9 Hz, 1H), 5.08–5.12 (d, J = 8.9 Hz, 1H), 6.55–6.58 (d, J = 7.26 Hz, 1H), 6.76–6.79 (d, J = 7.91 Hz, 1H), 6.92–7.04 (m, 2H), 7.11–7.19 (m, 7H), 7.40–7.43 (d, J = 8.25 Hz, 2H), 8.19–8.21 (d, J = 8.25 Hz, 1H), 9.22–9.32 (bs, 1H), HRFAB-MS: m/z 590.2704 for [M+H]⁺ (calcd. 590.2689 for $C_{33}H_{40}N_3O_5S$).

3-Hydroxy-2-methylbenzoyl-Apns-Dmt-NH-MPH (8b)

$[a]_D^6$ +28.82 (c = 0.17, CH_3OH), ¹H NMR (DMSO-d₆) δ: 1.47 (s, 3H), 1.56 (s, 3H), 1.82 (s, 3H), 2.67–2.87 (m, 2H), 3.06 (s, 3H), 4.41 (s, 2H), 4.49 (s, 1H), 5.02–5.06 (d, J = 8.91 Hz, 1H), 5.14–5.18 (d, J = 9.24 Hz, 1H), 6.54–6.57 (d, J = 7.26 Hz, 1H), 6.66–6.72 (t, J = 7.26 Hz, 1H), 6.76–6.78 (d, J = 7.58 Hz, 1H), 6.87–6.96 (m, 3H), 7.11–7.27 (m, 7H), 8.15–8.19 (d, J = 8.25 Hz, 1H), 9.35 (s, 1H), 10.12 (s,1H), HRFAB-MS: m/z 577.2492 for [M+H]⁺ (calcd. 577.2485 for $C_{31}H_{37}N_4O_5S$).

3-Hydroxy-2-methylbenzoyl-Apns-Dmt-NH-(2-OCH₃)Bz (8c)

$[a]_D^{7.5}$ 0.00 (c = 0.07, CH_3OH), ¹H NMR (DMSO-d₆) δ: 1.35 (s, 3H), 1.51 (s, 3H), 1.84 (s, 3H), 2.69–2.88 (m, 2H), 3.79 (s, 3H), 4.20–4.38 (m, 2H), 4.40–4.48 (m, 3H), 4.99–5.03 (d, J = 9.24, 1H), 5.12–5.16 (d, J = 9.24, 1H), 6.54–6.57 (d, J = 7.26 Hz, 1H), 6.76–6.94 (m, 4H), 7.14–7.33 (m, 7H), 8.12–8.15 (d, J = 8.24 Hz, 1H), 8.25–8.28 (m, 1H), 9.20–9.50 (bs, 1H), HRFAB-MS: m/z 592.2472 for [M+H]⁺ (calcd. 592.2481 for $C_{32}H_{38}N_3O_6S$).

3-Hydroxy-2-methylbenzoyl-Apns-Dmt-NH-(2-OC₂H₅)Bz (8d)

$[a]_D^{5.6}$ +20.32 (c = 0.123, CH_3OH), ¹H NMR (DMSO-d₆) δ: 1.33–1.38 (m, 6H), 1.51 (s ,3H), 1.83 (s, 3H), 2.76–2.88 (m, 2H), 4.00–4.05 (m, 2H), 4.14–4.49 (m, 5H), 5.00–5.03 (d, J = 9.24 Hz, 1H), 5.13–5.16 (d, J = 9.24 Hz, 1H), 6.53–6.56 (d, J = 7.26 Hz, 1H), 6.75–6.84 (m, 2H), 6.91–7.04 (m, 2H), 7.14–7.35 (m, 7H), 8.12–8.15 (d, J = 7.58 Hz, 1H), 8.20–8.30 (m, 1H), 9.35 (s, 1H), HRFAB-MS: m/z 606.2652 for [M+H]⁺ (calcd. 606.2638 for $C_{33}H_{40}N_3O_6S$).

3-Hydroxy-2-methylbenzoyl-Apns-Dmt-NH-Ind (8e)

$[a]_D^{4.2}$ +35.00 (c = 0.22, CH_3OH), ¹H NMR (DMSO-d₆) δ: 1.44 (s, 3H), 1.51 (s, 3H), 1.82 (s, 3H), 2.27–2.49 (m, 2H), 2.75–2.91 (m, 4H), 4.46–4.51 (m, 3H), 5.00–5.04 (m, 1H), 5.06–5.18 (m, 1H), 5.24–5.37 (m, 1H), 6.54–6.57 (d, J = 7.26 Hz, 1H), 6.76–6.79 (d, J = 7.91 Hz, 1H), 6.84–6.95 (m, 1H), 7.10–7.39 (m, 9H), 8.16–8.19 (t, J = 7.59 Hz, 1H), 8.33–8.39 (t, J = 8.91 Hz, 1H), 9.37 (bs, 1H), HRFAB-MS: m/z 588.2548 for [M+H]⁺ (calcd. 588.2532 for $C_{33}H_{38}N_3O_5S$).

3-Hydroxy-2-methylbenzoyl-Apns-Dmt-NH-Pip (8f)

$[a]_D^{4.5}$ +16.36 (c = 0.11, CH_3OH), ¹H NMR (DMSO-d₆) δ: 1.34 (s, 3H), 1.50 (s, 3H), 1.83 (s, 3H), 2.73–2.88 (m, 2H), 4.03–4.10 (m, 1H), 4.28–4.36 (m, 1H), 4.42–4.47 (d, J = 12.7 Hz, 3H), 4.99–5.03 (d, J = 9.24 Hz, 1H), 5.12–5.16 (d, J = 8.9 Hz, 1H), 5.90–5.96 (m, 2H), 6.54–6.57 (d, J = 7.26 Hz, 1H), 6.73–6.88 (m, 4H), 6.92–6.98 (t, J = 7.92 Hz, 1H), 7.16–7.33 (m, 5H), 8.11–8.14 (d, J = 7.92 Hz, 1H), 8.37–8.39 (t, J = 5.61 Hz, 1H), 9.20–9.60 (bs, 1H), HRFAB-MS: m/z 606.2269 for [M+H]⁺ (calcd. 606.2274 for $C_{32}H_{36}N_3O_7S$).

3-Hydroxy-2-methylbenzoyl-Apns-Dmt-NH-3-picolyl (8g)

$[a]_D^{5.8}$ +15.62 (c = 0.224, CH_3OH), ¹H NMR (DMSO-d₆) δ: 1.32 (s, 3H), 1.50 (s, 3H), 1.82 (s, 3H), 2.68–2.86 (m, 2H), 4.15–4.23 (m, 1H), 4.28–4.47 (m, 4H), 5.00–5.03 (d, J = 8.91, 1H), 5.13–5.17 (d, J = 9.23 Hz, 1H), 5.49–5.52 (d, J = 6.6 Hz, 1H), 6.53–6.56 (d, J = 7.26 Hz, 1H), 6.76–6.79 (d, J = 7.91 Hz, 1H), 6.90–6.98 (m, 1H), 7.13–7.31 (m, 6H), 7.67–7.70 (d, J = 7.58 Hz, 1H), 8.12–8.15 (d, J = 7.91 Hz, 1H), 8.39–8.53 (m, 3H), 9.38 (bs, 1H), HRFAB-MS: m/z 563.2341 for [M+H]⁺ (calcd. 563.2328 for $C_{30}H_{35}N_4O_5S$).

3-Hydroxy-2-methylbenzoyl-Apns-Dmt-NH-4-picolyl (8h)

$[a]_D^{7.5}$ +25.92 (c = 0.135, CH_3OH), ¹H NMR (DMSO-d₆) δ: 1.37 (s, 3H), 1.55 (s, 3H), 1.80 (s, 3H), 2.70–2.90 (m, 2H), 4.20–4.66 (m, 5H), 5.01–5.05 (d, J = 8.7 Hz, 1H), 5.15–5.19 (d, J = 8.9 Hz, 1H), 6.53–6.55 (d, J = 7.26 Hz, 1H), 6.73–6.76 (d, J = 7.9 Hz,1H), 6.86–6.92 (t, J = 7.83 Hz 1H), 7.05–7.32 (m, 4H), 7.66–7.68 (d, J = 5.74 Hz, 2H), 8.08–8.12 (d, J = 7.9 Hz, 1H), 8.26 (d, J = 1.7 Hz 1H), 8.56–8.60 (d, J = 6.26 Hz, 2H), 8.70–8.76 (m, 1H), 9.35–9.45 (bs, 1H), HRFAB-MS: m/z 563.2337 for [M+H]⁺ (calcd. 563.2328 for $C_{30}H_{35}N_4O_5S$).

3-Hydroxy-2-methylbenzoyl-Apns-Dmt-NH-1-Adam (8o)

$[a]_D^{8.5}$ +7.45 (c = 0.295, CH_3OH), ¹H NMR (DMSO-d₆) δ: 1.41 (s, 3H), 1.48 (s, 3H), 1.61 (s, 6H), 1.82–1.96 (m, 12H), 2.69–2.82 (m, 2H), 4.24–4.42 (m, 1H), 4.53 (s, 2H), 4.94–4.97 (d, J = 9.23 Hz, 1H), 5.15–5.18 (d, J = 8.25 Hz, 1H), 6.55–6.57 (d, J = 6.93 Hz, 1H), 6.76–6.79 (d, J = 7.58 Hz, 1H), 6.91–6.94 (m, 1H), 7.07–7.23 (m, 3H), 7.37–7.39 (d, J = 6.92 Hz, 2H), 7.49 (s, 1H), 8.22–8.25 (d, J = 8.25 Hz, 1H), 9.20–9.60 (bs, 1H), HRFAB-MS: m/z 606.3011 for [M+H]⁺ (calcd. 606.3002 for $C_{34}H_{44}N_3O_5S$).

3-Hydroxy-2-methylbenzoyl-Apns-Dmt-NH-2-Adam (8p)

$[a]_D^{0}$ +11.81 (c = 0.127, CH_3OH), ¹H NMR (DMSO-d₆) δ: 1.38 (s, 3H), 1.48–1.52 (m, 6H), 1.69–2.09 (m, 15H), 2.65–2.81 (m, 2H), 3.89 (s, 1H), 4.31–4.37 (m, 1H), 4.51 (s, 1H), 4.70 (s, 1H), 4.99–5.02 (d, J = 8.91 Hz, 1H), 5.13–5.16 (d, J = 8.58 Hz, 1H), 6.53–6.56 (d, J = 7.59 Hz, 1H), 6.76–6.78 (d, J = 7.25 Hz, 4H), 6.91–6.93 (t, J = 7.58 Hz, 1H), 7.08–7.32 (m, 5H), 7.81–7.84 (d, J = 6.26 Hz, 1H), 8.19–8.22 (d, J = 7.92 Hz, 1H), HRFAB-MS: m/z 606.3011 for [M+H]⁺ (calcd. 606.3002 for $C_{34}H_{44}N_3O_5S$).

HIV protease inhibition

HIV protease inhibition was determined by an HPLC method using S10 peptide (H-Lys-Ala-Arg-Val-Tyr*Phe(p-NO₂)-Glu-Ala-Nle-NH₂) as the enzyme substrate. The inhibitory potentials were tested at 50 nM concentration of the inhibitor. The assay protocol was followed as described by Mimoto et al. [15].

References

[1] A.Carrillo, K. D. Stewart, H. L. Sham, D. W. Norbeck, W. E. Kohlbrenner, J. M. Leonard, D. J. Kempf, A. Monna, J. Virol. 1998, 72, 7532–7541.

[2] L. Tong, S. Pav, S. Mui, D. Lamarre, C. Yoakim, P. Beaulieu, P. C. Anderson, Structure 1995, 3, 33–40.

[3] A. A. Bekhit, H. Matsumoto, H. M. M. Abdel-Rahman, T. Mimoto, S. Nojima, H. Takaku, T. Kimura, K. Akaji,

598   El-Koussi et al.

Arch. Pharm. Pharm. Med. Chem. 2004, 337, 587–598

Y. Kiso; "Peptide Science – Present and Future", Proceedings of the 1st International Peptide Symposium, Ed. Y. Shimonishi, Kluwer Academic Publishers, Dordrecht, 1999, pp. 660–661.

[4] R. S. Randad, L. Lubkowska, T. N. Bhat, S. Munshi, S. V. Gulnik, B. Yu, J. W. Erickson, Bioorg. Med. Chem. Lett. 1995, 5, 1707–1712.

[5] R. S. Randad, L. Lubkowska, A. M. Silva, D. M. A. Guerin, S. V. Gulnik, B. Yu, J. W. Erickson, Bioorg. Med. Chem. 1996, 4, 1471–1480.

[6] D. J. Kempf, C. A. Flentge, N. E. Wideburg, A. Saldivar, S. Vasavanonda, D. W. Norbeck, Bioorg. Med. Chem. Lett. 1995, 5, 2725–2728.

[7] Y. Kiso, S.Yamaguchi, H. Matsumoto, T. Mimoto, R. Kato, S. Nojime, H. Takaku, T. Fukkazawa, T. Kimura, K. Akaji, Arch. Pharm. Pharm. Med. Chem. 1998, 331, 87.

[8] M. S. Roger, H. B. Christina, J. Chromatogr. 1989, 475, 57.

[9] P. Ruelle, W. K. Ulrich, J. Pharm. Sci. 1998, 87, 987.

[10] M.Schutkowski, C. Mrestani-Klaus, K. Neubert, Int. J. Peptide Protein Res. 1995, 45, 257–265.

[11] D.Hudson, J. Org. Chem. 1988, 53, 617–624.

[12] T. Miyazawa, T. Yamada, S. Kuwata, Bull. Chem. Soc. Jpn. 1988, 61, 606–608.

[13] A. S. Kende, D. Scholz, J. Schneider, Synth. Commun. 1978, 8, 59–63.

[14] J. Dudash, Jr., J. Jiang, S. C. Mayer, M. M Joullie, Synth. Commun. 1993, 23, 349–356.

[15] T. Mimoto, R. Kato, H. Takaku, S. Nojima, K. Terashima, S. Misawa, T. Fukazawa, T. Ueno, H.Sato, M. Shintani, Y. Kiso, H. Hayashi, J. Med. Chem. 1999, 42, 1789–1802.

[16] H. M. M. Abdel-Rahman, Ph.D. Thesis, Assiut University, Egypt, 1999.

[17] Y. Kiso, Biopolymers (Peptide Science) 1996, 40, 235–244.

[18] M. M. Sheha, N. M. Mahfouz, H. Y. Hassan, A. F. Youssef, T. Mimoto, Y. Kiso, Eur. J. Med. Chem. 2000, 35, 887–894.

Design and synthesis of highly active Alzheimer's β-secretase (BACE1) inhibitors, KMI-420 and KMI-429, with enhanced chemical stability

Tooru Kimura,[a,b] Daisuke Shuto,[a] Yoshio Hamada,[a,b] Naoto Igawa,[a] Soko Kasai,[a] Ping Liu,[a] Koushi Hidaka,[a,b] Takashi Hamada,[a] Yoshio Hayashi[a,b] and Yoshiaki Kiso[a,b,*]

[a]Department of Medicinal Chemistry, Center for Frontier Research in Medicinal Science, Kyoto Pharmaceutical University, Yamashina-ku, Kyoto 607-8412, Japan
[b]21st Century COE Program, Kyoto Pharmaceutical University, Yamashina-ku, Kyoto 607-8412, Japan

Abstract—Recently, we reported potent and small-sized BACE1 inhibitors KMI-358 and KMI-370 in which the Glu residue is replaced by a β-N-oxalyl-DAP (L-α,β-diaminopropionyl) residue at the P_4 position. The β-N-oxalyl-DAP group is important for enhancing BACE1 inhibitory activity, but these inhibitors isomerized to α-N-oxalyl-DAP derivatives in solvents. Hence, we used a tetrazole moiety as a bioisostere of the free carboxylic acid of the oxalyl group. KMI-420 and KMI-429, containing a tetrazole ring, showed improved stability and potent enzyme inhibitory activity.
© 2004 Elsevier Ltd. All rights reserved.

1. Introduction

Amyloid β peptide (Aβ), which is the main component of senile plaques found in the brains of Alzheimer's disease (AD) patients,[1] is formed by proteolytic processing of amyloid precursor protein (APP).[2,3] Since BACE1 (β-site APP cleaving enzyme, β-secretase) triggers Aβ formation by cleaving at the N-terminus of the Aβ domain,[4–7] it is a molecular target for therapeutic intervention in AD.[8–11] Recently, we reported on the BACE1 inhibitors, KMI-300 (**1b**), -358 (**2b**), and -370 (**3b**)[12] (Fig. 1), which contained phenylnorstatine [Pns: (2R,3S)-3-amino-2-hydroxy-4-phenylbutyric acid] as a substrate transition-state mimic.[13,14] These inhibitors were designed from the octapeptide BACE1 inhibitor KMI-008[11] as the lead compound. However, inhibitors, **1b–3b**, have labile β-N-oxalyl-DAP residues (DAP: L-α,β-diaminopropionic acid) at the P_4 position. β-N-oxalyl-DAP is known as the neurotoxic constituent of the legume *Lathyrus sativus*,[15–17] which thermally isomerizes to an equilibrium mixture with α-N-oxalyl-DAP.[18,19]

Similarly, the compounds **1b–3b** are converted to α-N-oxalyl-DAP derivatives (Fig. 2), which show the low enzyme inhibitory activities, in aqueous and organic
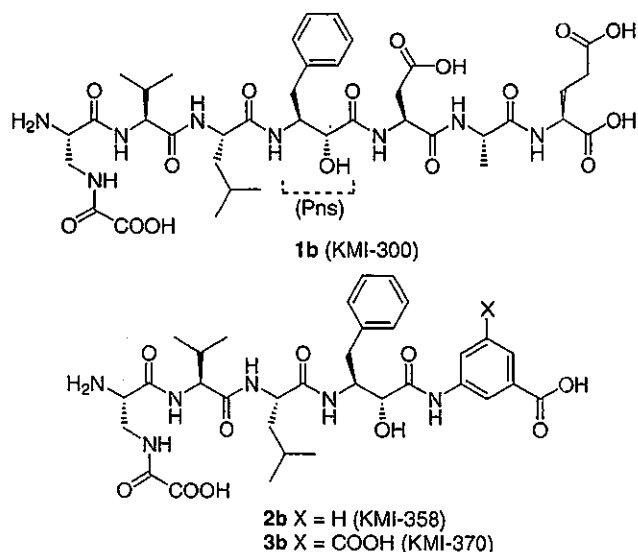

1b (KMI-300)

2b X = H (KMI-358)
3b X = COOH (KMI-370)

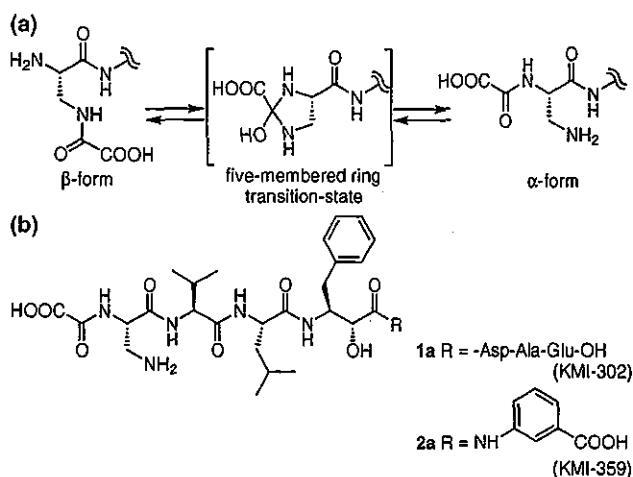Figure 1. Structure of BACE1 inhibitors containing β-oxalyl-DAP residue at the P_4 position.

Figure 2. (a) Isomerization of oxalyl-DAP derivatives. (b) Structure of BACE1 inhibitor's isomers containing α-oxalyl-DAP residue at the P4 position.
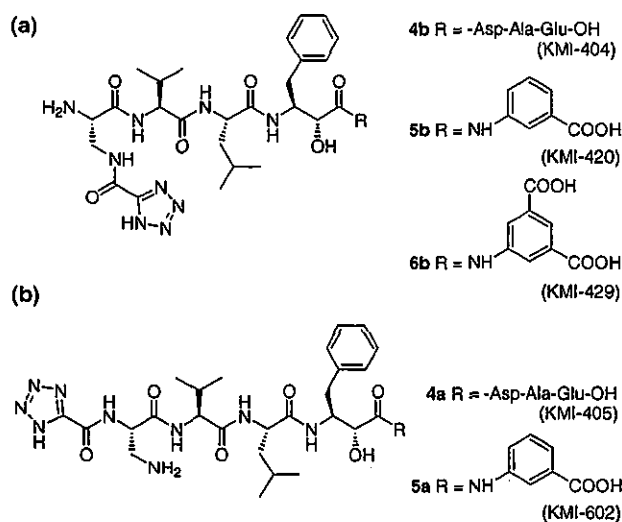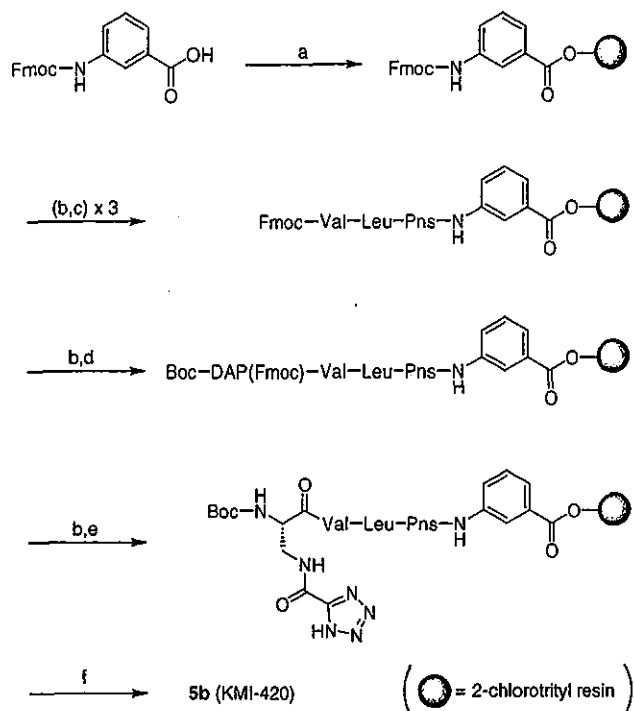

Figure 3. Structure of BACE1 inhibitors containing a tetrazole ring at the P4 position (a) and their α-isomers (b).

Scheme 1. Reagents and conditions: (a) 2-chlorotrityl chloride resin, DIPEA/DCM; (b) 20% piperidine/DMF; (c) Fmoc-AA-OH, DIPCDI, HOBt/DMF; (d) Boc-DAP(Fmoc)-OH, DIPCDI, HOBt/DMF; (e) 1H-tetrazole-5-carboxylic acid, DIPCDI, HOBt/DMF; (f) TFA, m-cresol, thioanisole.

solvents. To improve the stability of compounds 1b–3b, the oxalyl moiety was replaced with tetrazole carbonyl derivatives as a bioisostere[20] of carboxylic acid. Consequently, we found the tetrazole-containing BACE1 inhibitors 4b–6b (Fig. 3), with enhanced chemical stability and enzyme inhibitory activity.

2. Synthesis

BACE1 inhibitors (4b and 5b) and α-isomers (1a, 2a, 4a, and 5a) were synthesized by the 9-fluorenylmethoxycarbonyl (Fmoc)-based solid phase peptide synthesis as previously reported.[12] As an example, Scheme 1 shows the synthesis of 5b (KMI-420). Namely, the N-Fmoc-3-aminobenzoic acid was attached to 2-chlorotrityl chloride resin using diisopropylethylamine (DIPEA) in dichloromethane (DCM). The Fmoc group was removed with 20% piperidine in DMF and the peptide

bonds were formed using diisopropylcarbodiimide (DIPCDI) in the presence of 1-hydroxybenzotriazole (HOBt). The coupling of Boc-Pns-OH and aminobenzoyl resin was achieved using the same manner reported previously[12] without any problem. The DAP residue at the P4 position was introduced using N^α-Boc-N^β-Fmoc-L-2,3-diaminopropionic acid [Boc-DAP-(Fmoc)-OH]. The β-substituted DAP moiety in 4b (KMI-404) was introduced in a manner similar to that in 5b. However, for the α-substituted derivatives (1a, 2a, 4a and 5a), the DAP residue at the P4 position was introduced using N^β-Boc-N^α-Fmoc-L-2,3-diaminopropionic acid [Fmoc-DAP(Boc)-OH]. After peptide chain elongation, the 1H-tetrazole-5-carbonyl residue at the β-position of DAP was introduced using 1H-tetrazole-5-carboxylic acid. Finally, the peptide was cleaved from the resin by treatment with trifluoroacetic acid (TFA) in the presence of m-cresol and thioanisole. The crude peptide was purified by preparative RP-HPLC. On the other hand, the α-oxalyl residue at the P4 position in compounds 1a and 2a was introduced using oxalic acid mono-t-butyl ester.

Compound 6b (KMI-429), which contained 5-amino-isophthalic acid at the C-terminus, was synthesized by a traditional solution method (Scheme 2). Dibenzyl 5-aminoisophthalate was used as a starting compound and 1-ethyl-3-(3-dimethylaminopropyl)carbodiimide·HCl (EDC·HCl) in the presence of HOBt formed the peptide bonds. Boc and Fmoc groups were deprotected using 4 M HCl in dioxane and 20% diethylamine in DMF,
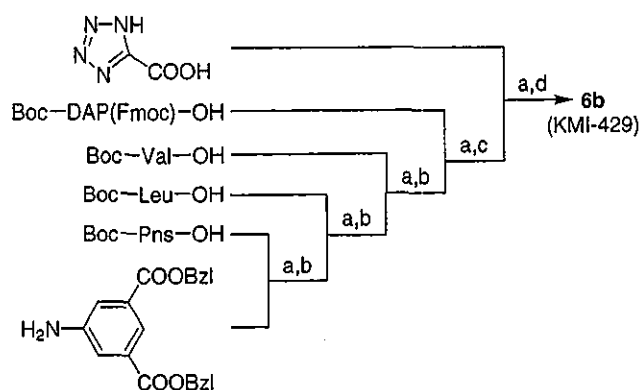
Scheme 2. Reagents and conditions: (a) EDC·HCl, HOBt/DMF; (b) 4M HCl/dioxane; (c) 20% Et₂NH/DMF; (d) TMS-Br, thioanisole, m-cresol/TFA.

respectively. The final deprotection of the Boc and benzyl groups using trimethylbromosilane (TMS-Br), thioanisole, and m-cresol in TFA and subsequent purification by preparative RP-HPLC gave the desired inhibitor 6b.

3. Results and discussion

3.1. Stability of KMI-300 (1b) and KMI-358 (2b)

Since the small-sized BACE1 inhibitors, 1b–3b, showed unstable features, we investigated the mechanism and kinetics for the unstability. It seems that by-products are formed from the isomerization via oxalyl migration. Thus we synthesized the α-oxalyl isomers 1a and 2a, corresponding to 1b and 2b, respectively, which contained a β-oxalyl DAP group. The HPLC analysis and mass spectra showed that compounds 1a and 2a are identical to the by-products of 1b and 2b, respectively. Next, we monitored the isomerization of 1b, 2b, 1a, and 2a in various solvents by HPLC. Compounds 1b, 2b, 1a, and 2a showed a time-dependent isomerization to an equilibrium mixture (Fig. 4). A slower migration is observed in an aqueous solvent, for example, PBS (phosphate-buffered saline, pH 7.4), than in organic solvents such as MeOH and DMSO. Though the β-isomers (1b and 2b) and α-isomers (1a and 2a), respectively, were isomerized to reach the same equilibrium ratio under the same conditions, the equilibrium ratio and migration rate are dependent on the solvents and the chemical structure of the compounds. Abegaz et al. indicated that the migration rate of oxalyl-DAPs is influenced by the rotamers in the solvents.[19] The difference between α-N to β-N and β-N to α-N oxalyl migration rates might determine the equilibrium ratio. Recently, we reported on the water-soluble prodrugs of HIV-1 protease inhibitors based on O → N intramolecular acyl migration[21–24] and the kinetic study in different solvents.[23,24] These prodrugs could be converted to the parent drugs via a 'five-membered ring intermediate' under physiological conditions. This mechanism via a five-membered ring intermediate, permitted two equilibrium constants, is consistent with the above findings.
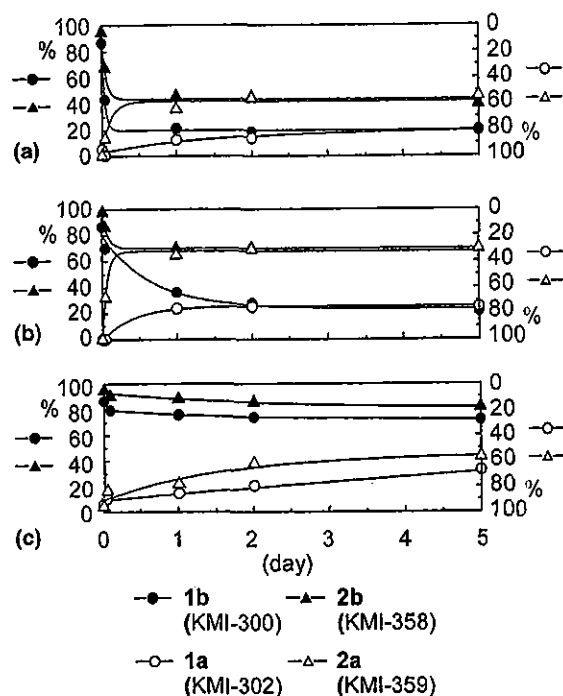

Figure 4. Stability of KMI compounds containing α- or β-oxalyl-DAP residue at the P₄ position in MeOH (a), DMSO (b), or pH 7.4 PBS (c). To unify the β-isomer's ratio to upward direction in the graph, the y-axis direction of α-isomers (1a and 2a) was reversed.

3.2. Stability and BACE1 inhibitory activity of KMI-404 (4b), KMI-420 (5b), and KMI-429 (6b)

To improve the stability of BACE1 inhibitors 1b–3b, we replaced the oxalyl group with the 1H-tetrazole-5-carbonyl group. The stability of the tetrazole-type BACE1 inhibitors 4b (KMI-404), 5b (KMI-420), and 6b (KMI-429), which correspond to 1b–3b, respectively, was verified by HPLC. 4b–6b showed no isomerization in PBS (pH 7.4), MeOH and DMSO over a period up to 5 days.

As shown in Table 1, the BACE1 inhibitory activities of β-N-tetrazole-5-carbonyl-type inhibitors 4b–6b were enhanced over β-N-oxalyl-type inhibitors 1b–3b, respectively. The α-isomers 1a, 2a, 4a, and 5a showed weaker BACE1 inhibitory activities than the corresponding

Table 1. BACE1 inhibitory activity

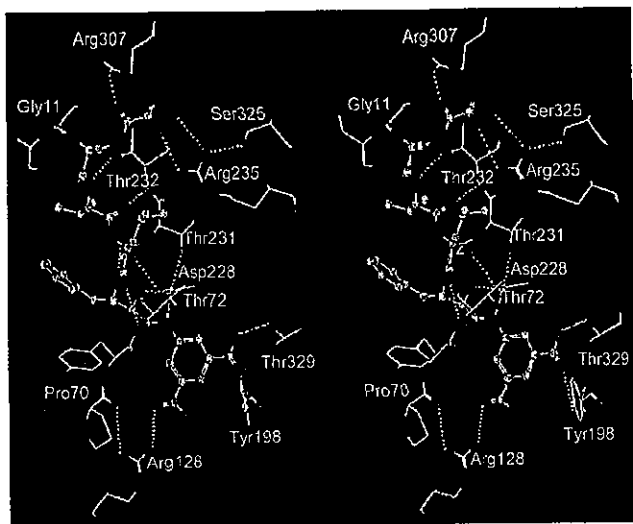| Compd (KMI No.)	BACE1 inhibition (%)		IC₅₀ (nM)
	At 2 µM	At 0.2 µM	
1b (KMI-300)	96.7	57.6	84
2b (KMI-358)	98.4	85.5	16
3b (KMI-370)	99.8	96.7	4.7
1a (KMI-302)	75.2	—	—
2a (KMI-359)	87.9	58.6	—
4b (KMI-404)	93.0	73.1	—
5b (KMI-420)	99.0	87.1	8.2
6b (KMI-429)	100	98.1	3.9
4a (KMI-405)	23.2	—	—
5a (KMI-602)	~0	—	—

Figure 5. Modeled structure of BACE1 (skeleton model)-6b KMI-429 (ball and stick model) complex based on the crystal structure of BACE1 bound to OM99-2.[25] White dashed lines indicate hydrogen bonds to the inhibitor.

β-isomers 1b, 2b, 4b, and 5b, respectively. As compared with 4a and 5a showing no isomerization, relatively high activities of 1a and 2a are probably due to the activities of the corresponding β-isomers 1b and 2b formed partially by the isomerization of 1a and 2a during incubation in this assay. The IC$_{50}$ values of 5b and 6b were improved as compared to those of 2b and 3b, respectively.

As shown in Figure 5, the tetrazole ring, which is slightly larger than a carboxylic acid, allows the formation of hydrogen bonds to both Arg235 and Arg307 residues of BACE1. Moreover, as previously described,[12] compound 3b, which contains two carboxylic groups at the P$_1$' position, exhibited a higher BACE1 inhibitory activity than compound 2b, which contains a carboxylic group at the P$_1$' position. Similarly, compound 6b exhibited higher BACE1 inhibitory activity than compound 5b. The two carboxylic groups at the P$_1$' position of compound 6b allow the formation of rigid hydrogen bonds in BACE1 as shown in Figure 5. As described above, it seems that the acidic functional groups at the P$_4$ (as an isostere of the carboxylic group) and P$_1$' sites are important for enhancing BACE1 inhibitory activity.

4. Conclusion

We found that replacing the labile β-N-oxalyl-DAP group of 2b (KMI-358) and 3b (KMI-370) with a 1H-tetrazole-5-carbonyl group resulted in more potent and chemically stable BACE1 inhibitors, 5b (KMI-420) and 6b (KMI-429). Replacing carboxylic acid with bio-isostere, such as tetrazole ring, is expected to enhance the membrane permeability, which is considered to be a key issue in developing AD's drugs based on the 'amyloid hypothesis'.[26–29]

References and notes

1. Selkoe, D. J. Neuron 1991, 6, 487.
2. Selkoe, D. J. Nature 1999, 399, A23.
3. Sinha, S.; Lieberburg, I. Proc. Natl. Acad. Sci. U.S.A. 1999, 96, 11049.
4. Vassar, R.; Bennett, B. D.; Babu-Khan, S.; Kahn, S.; Mendiaz, E. A.; Denis, P.; Teplow, D. B.; Ross, S.; Amarante, P.; Loeloff, R.; Luo, Y.; Fisher, S.; Fuller, J.; Edenson, S.; Lile, J.; Jarosinski, M. A.; Biere, A. L.; Curran, E.; Burgess, T.; Louis, J. C.; Collins, F.; Treanor, J.; Rogers, G.; Citron, M. Science 1999, 286, 735.
5. Yan, R.; Bienkowski, M. J.; Shuck, M. E.; Miao, H.; Tory, M. C.; Pauley, A. M.; Brashier, J. R.; Stratman, N. C.; Mathews, W. R.; Buhl, A. E.; Carter, D. B.; Tomaselli, A. G.; Parodi, L. A.; Heinrikson, R. L.; Gurney, M. E. Nature 1999, 402, 533.
6. Sinha, S.; Anderson, J. P.; Barbour, R.; Basi, G. S.; Caccavello, R.; Davis, D.; Doan, M.; Dovey, H. F.; Frigon, N.; Hong, J.; Jacobson-Croak, K.; Jewett, N.; Keim, P.; Knops, J.; Lieberburg, I.; Power, M.; Tan, H.; Tatsuno, G.; Tung, J.; Schenk, D.; Seubert, P.; Suomensaari, S. M.; Wang, S.; Walker, D.; Zhao, J.; McConlogue, L.; John, V. Nature 1999, 402, 537.
7. Hussain, I.; Powell, D.; Howlett, D. R.; Tew, D. G.; Meek, T. D.; Chapman, C.; Gloger, I. S.; Murphy, K. E.; Southan, C. D.; Ryan, D. M.; Smith, T. S.; Simmons, D. L.; Walsh, F. S.; Dingwall, C.; Christie, G. Mol. Cell. Neurosci. 1999, 14, 419.
8. (a) Ghosh, A. K.; Shin, D.; Downs, D.; Koelsch, G.; Lin, X.; Ermolieff, J.; Tang, J. J. Am. Chem. Soc. 2000, 122, 3522; (b) Ghosh, A. K.; Bilcer, G.; Harwood, C.; Kawahara, R.; Shin, D.; Hussain, K. A.; Hong, L.; Loy, J. A.; Nguyen, C.; Koelsch, G.; Ermolieff, J.; Tang, J. J. Med. Chem. 2001, 44, 2865.
9. Tung, J. S.; Davis, D. L.; Anderson, J. P.; Walker, D. E.; Mamo, S.; Jewett, N.; Hom, R. K.; Sinha, S.; Thorsett, E. D.; John, V. J. Med. Chem. 2002, 45, 259.
10. Tamamura, H.; Kato, T.; Otaka, A.; Fujii, N. Org. Biomol. Chem. 2003, 1, 2468.
11. Shuto, D.; Kasai, S.; Kimura, T.; Liu, P.; Hidaka, K.; Hamada, T.; Shibakawa, S.; Hayashi, Y.; Hattori, C.; Szabo, B.; Ishiura, S.; Kiso, Y. Bioorg. Med. Chem. Lett. 2003, 13, 4273.
12. Kimura, T.; Shuto, D.; Kasai, S.; Liu, P.; Hidaka, K.; Hamada, T.; Hayashi, Y.; Hattori, C.; Asai, M.; Kitazume, S.; Saido, T. C.; Ishiura, S.; Kiso, Y. Bioorg. Med. Chem. Lett. 2004, 14, 1527.
13. Mimoto, T.; Imai, J.; Tanaka, S.; Hattori, N.; Takahashi, O.; Kisanuki, S.; Nagano, Y.; Shintani, M.; Hayashi, H.; Akaji, K.; Kiso, Y. Chem. Pharm. Bull. 1991, 39, 2465.
14. Mimoto, T.; Imai, J.; Tanaka, S.; Hattori, N.; Kisanuki, S.; Akaji, K.; Kiso, Y. Chem. Pharm. Bull. 1991, 39, 3088.
15. Murti, V. V. S.; Seshadri, T. R.; Venkitasubramanian, T. A. Phytochemistry 1964, 3, 73.
16. Rao, S. L. N.; Adiga, P. R.; Sarma, P. S. Biochemistry 1964, 3, 432.

17. Spencer, P. S.; Roy, D. N.; Ludolph, A.; Hugon, J.; Dwivedi, M. P.; Schaumburg, H. H. *Lancet* **1986**, *11*, 1066.

18. Bell, E. A.; O'Donovan, J. P. *Phytochemistry* **1966**, *5*, 1211.

19. Abegaz, B. M.; Nunn, P. B.; De Bruyn, A.; Lambein, F. *Phytochemistry* **1993**, *33*, 1121.

20. Kohara, Y.; Kubo, K.; Imamiya, E.; Wada, T.; Inada, Y.; Naka, T. *J. Med. Chem.* **1996**, *39*, 5228.

21. Kiso, Y.; Matsumoto, H.; Yamaguchi, S.; Kimura, T. *Lett. Pept. Sci.* **1999**, *6*, 275.

22. Hamada, Y.; Ohtake, J.; Sohma, Y.; Kimura, T.; Hayashi, Y.; Kiso, Y. *Bioorg. Med. Chem.* **2002**, *10*, 4155.

23. Hamada, Y.; Matsumoto, H.; Kimura, T.; Hayashi, Y.; Kiso, Y. *Bioorg. Med. Chem. Lett.* **2003**, *13*, 2727.

24. Hamada, Y.; Matsumoto, H.; Yamaguchi, S.; Kimura, T.; Hayashi, Y.; Kiso, Y. *Bioorg. Med. Chem.* **2004**, *12*, 159.

25. Hong, L.; Koelsch, G.; Lin, X.; Wu, S.; Terzyan, S.; Ghosh, A. K.; Zhang, X. C.; Tang, J. *Science* **2000**, *290*, 150.

26. Sipe, J. D. *Annu. Rev. Biochem.* **1992**, *61*, 947.

27. Selkoe, D. J. *Ann. N.Y. Acad. Sci.* **2000**, *924*, 17.

28. Steiner, H.; Capell, A.; Leimer, U.; Haass, C. *Eur. Arch. Psychiatric Clin. Neurosci.* **1999**, *249*, 266.

29. Selkoe, D. J. *Ann. Med.* **1989**, *21*, 73.

High Level Expression of Human Immunodeficiency Virus Type-1 Vif Inhibits Viral Infectivity by Modulating Proteolytic Processing of the Gag Precursor at the p2/Nucleocapsid Processing Site*

Hirofumi Akari‡§, Mikako Fujita¶, Sandra Kao‡, Mohammad A. Khan‡, Miranda Shehu-Xhilaga‡, Akio Adachi¶, and Klaus Strebel‡∥

From the ‡Laboratory of Molecular Microbiology, NIAID, National Institutes of Health, Bethesda, Maryland 20892-0460, §Tsukuba Primate Center for Medical Science, The National Institute of Infectious Diseases, Ibaraki 305-0843, Japan, and the ¶Department of Virology, The University of Tokushima Graduate School of Medicine, Tokushima 770-8503, Japan

The human immunodeficiency virus type-1 Vif protein has a crucial role in regulating viral infectivity. However, we found that newly synthesized Vif is rapidly degraded by cellular proteases. We tested the dose dependence of Vif in non-permissive H9 cells and found that Vif, when expressed at low levels, increased virus infectivity in a dose-dependent manner. Surprisingly, however, the range of Vif required for optimal virus infectivity was narrow, and further increases in Vif severely reduced viral infectivity. Inhibition of viral infectivity at higher levels of Vif was cell type-independent and was associated with an accumulation of Gag-processing intermediates. Vif did not act as a general protease inhibitor but selectively inhibited Gag processing at the capsid and nucleocapsid (NC) boundary. Identification of Vif variants that were efficiently packaged but were unable to modulate Gag processing suggests that Vif packaging was necessary but insufficient for the production of 33- and 34-kDa processing intermediates. Interestingly, these processing intermediates, like Vif, associated with viral nucleoprotein complexes more rigidly than mature capsid and NC. We conclude that virus-associated Vif inhibits processing of a subset of Gag precursor molecules at the p2/NC primary cleavage site. Modulation of processing of a small subset of Gag molecules by physiological levels of Vif may be important for virus maturation. However, the accumulation of such processing intermediates at high levels of Vif is inhibitory. Thus, rapid intracellular degradation of Vif may have evolved as a mechanism to prevent such inhibitory effects of Vif.

The human immunodeficiency virus type-1 (HIV-1)[1] Vif protein is essential for viral replication in non-permissive cells such as primary CD4+ T lymphocytes and macrophages as well as some T cell lines including H9 and CEM cells (for review, see

¹ The abbreviations used are: HIV-1, human immunodeficiency virus type-1; NC, nucleocapsid; CA, capsid; VSV-G, vesicular stomatitis virus glycoprotein G; MA, matrix; CHAPS, 3-[(3-cholamidopropyl)dimethylammonio]-1-propanesulfonic acid; PR, protease.

Refs. 1 and 2). Vif-defective viruses produced from non-permissive cells are defective at an early postentry step of infection and are unable to complete reverse transcription and integration (3–9). In fibroblasts and most T cell lines, however, Vif is not required for the production of infectious HIV-1. This cell type-dependent requirement for Vif implied the involvement of host factor(s). Indeed, the recent identification of CEM15 (APOBEC3G) as a cellular inhibitor of HIV replication (10) confirmed earlier speculations on the existence of an inhibitory factor in non-permissive cell types (11, 12). APOBEC3G was subsequently found to induce hypermutation of the HIV genome by deaminating cytidine residues on the viral minus-strand cDNA resulting in the introduction of guanosine to adenosine mutations in the HIV genome (13–16). Subsequent reports suggested a role of Vif in the inhibition of APOBEC3G packaging into virus particles (17–21). The mechanism of APOBEC3G exclusion from virions, however, remains under investigation. Some reports suggest that Vif induces degradation of APOBEC3G (20, 21), whereas others report an effect on APOBEC3G translation (17, 19) or both (18).

While most current models propose an intracellular interaction of Vif with APOBEC3G, Vif is also packaged into virions. Virus particles produced from acutely infected cells incorporate 30–100 copies of Vif (22). In fact, packaging of Vif is specific and requires the interaction of Vif with the viral genomic RNA and the nucleocapsid (NC) domain of the Gag precursor (23). Moreover, virus-associated Vif is partially cleaved by the viral protease (PR) (24). Interestingly, mutations at the processing site that inhibited Vif processing inhibited Vif function, whereas mutations that did not interfere with Vif processing also did not affect Vif function (24). While these findings suggested an important role of virus-associated Vif in virions (24), its specific role remains under investigation.

In the current study we report that newly synthesized Vif is rapidly degraded in transiently transfected HeLa cells with a half-life of less than 30 min. We found that the presence or absence of APOBEC3G had no significant effect on the degradation kinetics of Vif. Based on recent reports demonstrating an interaction of Vif with APOBEC3G (17, 21, 25), we postulated that Vif enhances viral infectivity in a dose-dependent and saturable manner. Accordingly, increasing levels of Vif were expected to result in an increase in viral infectivity reaching a plateau of maximal infectivity once saturating amounts of Vif were reached or exceeded. Furthermore, increasing the amounts of Vif in permissive cell types was not expected to affect viral infectivity, as virus production in such cell types is Vif-independent due to the lack of APOBEC3G in such cells. As expected, physiological expression of Vif increased viral infec-

tivity in non-permissive cell types in a dose-dependent manner. Surprisingly, however, the amounts of Vif required for maximal effect exhibited a narrow window, and further increases in Vif levels did *not* result in a plateau of maximal viral infectivity but instead increasingly suppressed viral infectivity irrespective of the producer cell type. We investigated the mechanistic basis of this phenomenon and found that Vif suppresses processing of the Gag precursor at the p2/NC primary cleavage site. The resulting accumulation of 33- and 34-kDa Gag intermediates composed of CA-p2-NC and CA-p2-NC-p1 was found to inhibit viral infectivity. These results provide evidence that virus-associated Vif has the ability to interact with Gag precursor molecules and to modulate Gag maturation. However, Gag maturation is a highly ordered process, and accumulation of excessive amounts of processing intermediates due to high level expression of Vif is detrimental to virus infectivity.

EXPERIMENTAL PROCEDURES

Plasmids—The full-length HIV-1 molecular clone pNL4-3 was used for the production of wild type infectious virus (26). Construction of its variants pNL43-K1 (Env-defective) or pNL4-3vif(−) (Vif-defective) was described previously (27, 28). An Env- and Vif-defective variant, pNL43-K1.vif(−), was constructed by introducing a frameshift mutation in *env* at a KpnI site in pNL4-3vif(−). Plasmid pHCMV-G contains the vesicular stomatitis virus glycoprotein G (VSV-G) gene expressed from the immediate early gene promoter of human *cytomegalovirus* (29) and was used for the production of VSV-G pseudotypes. Construction of the APOBEC3G expression vector pHIV-Apo3G is described elsewhere (19). Expression of APOBEC3G from pHIV-Apo3G is under the control of the HIV-1 long terminal repeat and thus requires Tat for expression. For expression of Vif in *trans*, the subgenomic expression vector pNL-A1 (30) was used. A Vif-defective variant of pNL-A1, pNL-A1vif(−), was used as a control. Vif deletion mutants VifΔD (deletion of residues 23–43), VifΔF (deletion of residues 23–74), and VifΔI (deletion of residues 4–45) were created by two-step PCR amplification. PCR products were column-purified; appropriate pairs were mixed at equimolar ratios and used as templates for a second round of amplification using flanking primers. Final PCR products were cloned into pNL-A1 between the BssHII and EcoRI sites.

Cells—H9 and LuSIV cells were cultured in RPMI 1640 medium supplemented with 10% fetal bovine serum, L-glutamine, and antibiotics. HeLa cells were maintained in complete Dulbecco's modified Eagle's medium supplemented with 10% fetal bovine serum, L-glutamine, and antibiotics.

Transfection and Analysis of Viral Proteins—H9 cells (4×10^6) were transfected by electroporation with 10 μg each of pNL43-K1 or pNL43-K1.vif(−) and 10 μg of pNL-A1 or pNL-A1vif(−). The culture supernatants were harvested 24 h after transfection, filtered through 0.45-μm filters, and concentrated by ultracentrifugation through 20% sucrose for 1 h at 25,000 rpm using an SW41 rotor (Beckman Instruments). Alternatively, HeLa cells (5×10^5) were transfected with 2 μg each of variants of pNL4-3 and pNL-A1 using LipofectAMINE PLUS™ (Invitrogen). Culture supernatants and cells were harvested 24 h later. Cell and viral lysates were analyzed by immunoblotting as described previously (23) using an HIV-1-infected patient serum (APS) and antibodies against Vif (28), NC (kindly provided by Robert Gorelick), reverse transcriptase (Intracell), p24 capsid, and matrix (MA) (provided by S. Zolla-Pazner and P. Spearman, respectively, and obtained through the National Institutes of Health AIDS Research and Reference Reagent Program (31, 32)).

Pulse/Chase Analysis of Vif—Transfected cells were metabolically labeled for 10 min with [³⁵S]methionine (2 mCi/ml; ICN Biomedical, Inc., Costa Mesa, CA). After the labeling, cells were washed once with phosphate-buffered saline to remove free isotope and suspended in complete RPMI containing all amino acids and 10% fetal bovine serum. Cells were incubated for various times at 37 °C as indicated in the text. Cells were then pelleted and stored at −80 °C. Cell pellets were subsequently extracted with CHAPS buffer (50 mM Tris-hydrochloride, pH 8.0, 5 mM EDTA, 100 mM NaCl, and 0.5% (v/v) CHAPS (3-[(3-cholamidopropyl)dimethylammonio]-1-propanesulfonic acid)) supplemented with 0.2% deoxycholate, incubated on ice for 5 min, vortexed, and pelleted for 3 min at 15,000 × *g*. Proteins present in the supernatant were used for immunoprecipitation with a Vif-specific polyclonal antibody (Vif93) (28). Immunoprecipitated proteins were solubilized by
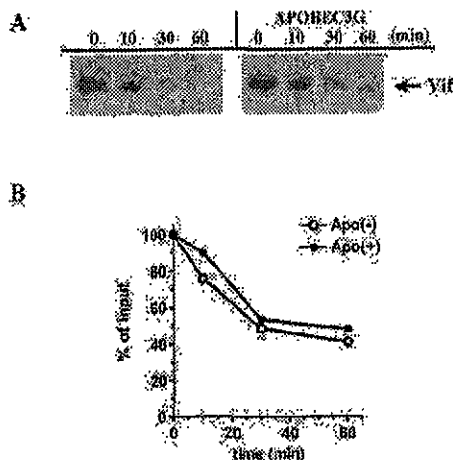

FIG. 1. **Newly synthesized Vif is rapidly degraded.** *A*, HeLa cells were transfected with pNL-A1 (4 μg) and a control vector, pHIV-T4 (1 μg) or pNL-A1 (4 μg) plus pHIV-Apo3G (1 μg). Cells were collected 24 h after transfection, labeled for 10 min with [³⁵S]methionine, and chased for up to 60 min as indicated *above the lanes*. Cell lysates were prepared as described under "Experimental Procedures" and precipitated with a Vif-specific polyclonal antibody. Vif proteins were identified by SDS-PAGE followed by fluorography. *B*, Vif-specific bands shown in *A*, respectively, were quantified using a Fuji BAS 2000 Phospho-Imager. Signals were calculated relative to the input value (time 0 = 100%) and plotted as a function time.

boiling in sample buffer and separated by SDS-PAGE. Radioactive bands were visualized by fluorography, and quantitation was performed using a Fuji BAS 2000 Bio-Image analyzer.

Single-round Viral Infectivity Analysis—Virus stocks derived from transfected H9 or HeLa cells were used for the infection of LuSIV indicator cells (33). To increase the sensitivity of the assay, viruses were pseudotyped with the vesicular stomatitis virus glycoprotein G. Unlike Nef defects, VSV-G pseudotyping does not rescue Vif defects (3, 34). LuSIV cells (5×10^5) were infected in a 24-well plate with 200–400 μl of *unconcentrated* virus supernatants. Cells were incubated for 24 h at 37 °C. Cells were then harvested and lysed in 150 μl of Promega 1× reporter lysis buffer (Promega Corp., Madison, WI). To determine the luciferase activity in the lysates, 50 μl of each lysate were combined with luciferase substrate (Promega Corp.) by automatic injection, and light emission was measured for 10 s at room temperature in a luminometer (Optocomp II, MGM Instruments, Hamden, CT).

Step Gradient Analysis—Concentrated virus preparations were treated with 0.1% Triton X-100 (final concentration) and subjected to fractionation by centrifugation through a 20%/60% sucrose step gradient as described previously (23). Three equal fractions were collected as depicted in Fig. 5; the top fraction (fraction 1) contains detergent-soluble viral proteins, fraction 2 is a buffer fraction and should not contain significant amounts of any viral proteins, and fraction 3 contains viral core components that are resistant to extraction with Triton X-100. Aliquots of each fraction were analyzed for viral proteins by immunoblotting.

RESULTS

Newly Synthesized Vif Is Rapidly Degraded—Recent work proposed that Vif induces proteasome-dependent degradation of APOBEC3G (20, 21, 25). Although we and others were unable to verify such Vif-dependent degradation of APOBEC3G (17, 19), we nevertheless wanted to assess the possible impact of APOBEC3G on Vif stability. To address this question, we performed pulse/chase analyses in transiently transfected HeLa cells (Fig. 1). To ascertain coexpression of Vif and APOBEC3G in the same cells, Vif was expressed from the subgenomic expression vector pNL-A1 (30), and APOBEC3G was expressed from the Tat-dependent vector pHIV-Apo3G (19). Transfected HeLa cells were labeled for 10 min with [³⁵S]methionine and chased for up to 60 min as described under "Experimental Procedures." As can be seen in Fig. 1A, Vif was rapidly degraded both in the absence and presence of